iScience

CellPress
OPEN ACCESS

Article

Mitochondrial Superoxide Dismutase Specifies Early Neural Commitment by Modulating Mitochondrial Dynamics

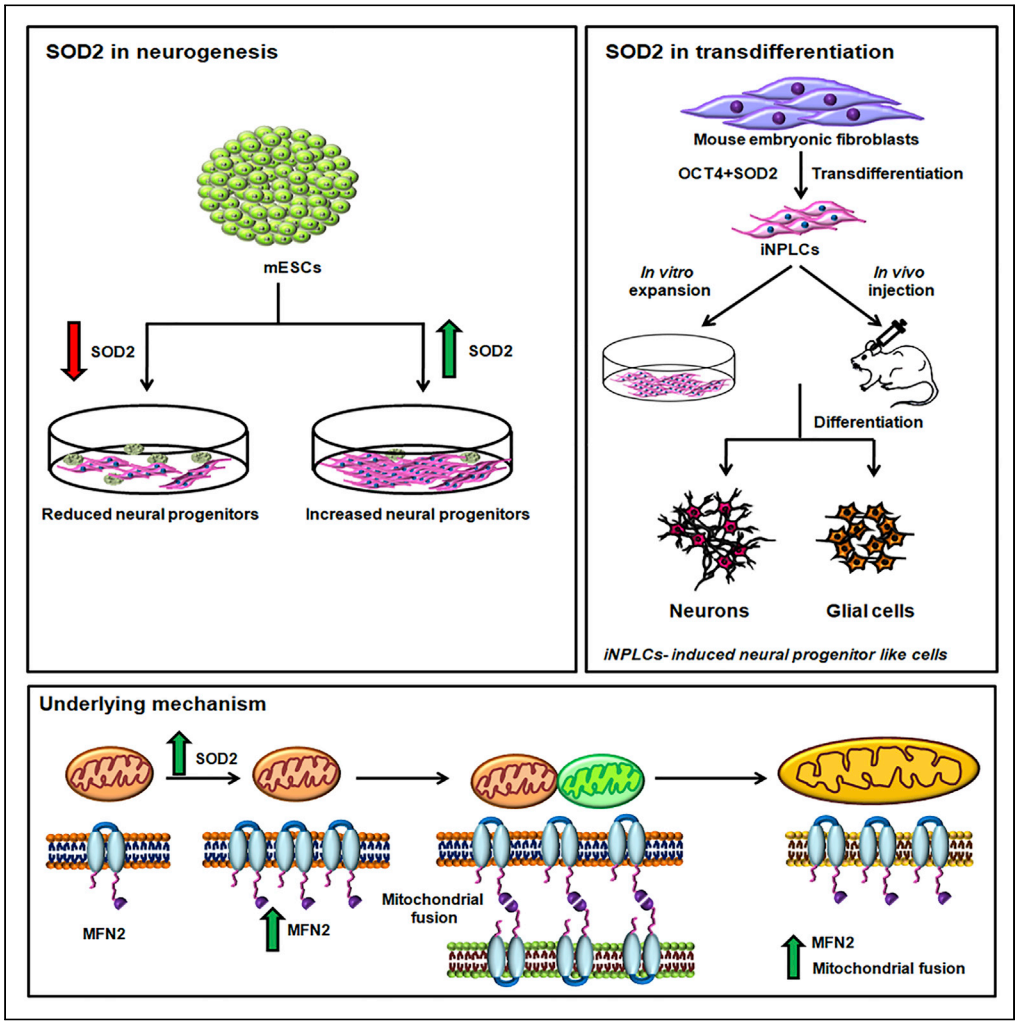

Smitha Bhaskar, Preethi Sheshadri, Joel P. Joseph, Chandrakanta Potdar, Jyothi Prasanna, Anujith Kumar

anujith.kumar@manipal.edu

HIGHLIGHTS

SOD2 is essential for early neural differentiation of mESCs

Up-regulation of MFN2, but not MFN1, underlies SOD2-mediated neurogenesis

Antioxidant enzymatic activity of SOD2 is dispensable for mitochondrial fusion

Overexpression of SOD2 with OCT4 transdifferentiate MEFs to iNPLCs

Bhaskar et al., iScience 23, 101564
October 23, 2020
https://doi.org/10.1016/j.isci.2020.101564

iScience

CellPress
OPEN ACCESS

Article

Mitochondrial Superoxide Dismutase Specifies Early Neural Commitment by Modulating Mitochondrial Dynamics

Smitha Bhaskar,[1,2] Preethi Sheshadri,[1,2] Joel P. Joseph,[1] Chandrakanta Potdar,[1] Jyothi Prasanna,[1] and Anujith Kumar[1,3,*]

SUMMARY

Studies revealing molecular mechanisms underlying neural specification have majorly focused on the role played by different transcription factors, but less on non-nuclear components. Earlier, we reported mitochondrial superoxide dismutase (SOD2) to be essential for self-renewal and pluripotency of mouse embryonic stem cells (mESCs). In the present study, we found SOD2 to be specifically required for neural lineage, but not the meso- or endoderm specification. Temporally, SOD2 regulated early neural genes, but not the matured genes, by modulating mitochondrial dynamics—specifically by enhancing the mitochondrial fusion protein Mitofusin 2 (MFN2). Bio-complementation strategy further confirmed SOD2 to enhance mitochondrial fusion process independent of its antioxidant activity. Over-expression of SOD2 along with OCT4, but neither alone, transdifferentiated mouse fibroblasts to neural progenitor-like colonies, conclusively proving the neurogenic potential of SOD2. In conclusion, our findings accredit a novel role for SOD2 in early neural lineage specification.

INTRODUCTION

Neurogenesis is an intricate developmental process that occurs as early as E10 in mice (Martynoga et al., 2012). The process includes a series of events including the formation of neural progenitor cells and their proliferation, migration, further differentiation, and commitment to form a functional circuitry of neurons across the brain (Stiles and Jernigan, 2010). Although the existence of neural stem cells (NSCs) in humans is highly debated, there is abundant evidence to support the existence of NSCs and neurogenesis in adult rodents (Eriksson et al., 1998; Toni et al., 2007). NSCs in adult brain are predominantly present in the sub-ventricular zone (SVZ) of the lateral ventricles and in the hippocampal dentate gyrus region (Alvarez-buylla and Garcı, 2002; Bond et al., 2015). Various intrinsic and extrinsic factors including transcription factors (TFs), epigenetic modulators, neurotropic factors, and neurogenic niche govern the generation and commitment of neurons in the developing brain.

Being a highly organized and energy-demanding process, neurogenesis requires active involvement of dynamic organelles like mitochondria to provide unlimited supply of energy (Agostini et al., 2016; Arrázola et al., 2019; Beckervordersandforth et al., 2017). During the course of energy production, mitochondria release superoxide radicals, which are further converted to hydrogen peroxide (Turrens, 2003). Mitochondrial SOD2, also known as manganese superoxide dismutase, is the major superoxide scavenging enzyme residing in the mitochondrial matrix (Wang et al., 2018). Upon selective knockdown of SOD2 in adult mice, although liver and other endocrine organs did not show any abnormality, the animal developed cardiomyopathy and severe damage in the brain leading to death within 3 weeks (Oh et al., 2012). Specific knockout of SOD2 in the brain also leads to encephalopathy and consequent death of the mice perinatally (Izuo et al., 2015). SOD2 level is highest in the central nervous system and is profusely expressed during early neural development, at as early as E7.5–8.5 in mice (Yon et al., 2011). Neural protection obtained by mitochondrial deacetylase SIRT3 has also been reported to be due to increased expression of SOD2 (Cheng et al., 2016). Increased SOD2 levels have also relieved the symptoms of Alzheimer's (Massaad et al., 2009) and Parkinson's disease (Klivenyi et al., 1998) in mouse models. Although the neuroprotective role of SOD2 is well appreciated, its role in neural lineage determination remains elusive.

[1]Manipal Institute of Regenerative Medicine, Manipal Academy of Higher Education, Allalasandra, Yelahanka, Bengaluru, 560065 Karnataka, India

[2]These authors contributed equally

[3]Lead Contact

*Correspondence: anujith.kumar@manipal.edu

https://doi.org/10.1016/j.isci.2020.101564

Recent studies revealed mitochondrial dynamics to be one of the key regulators of neural fate specification. Variation in mitochondrial mass and structure, changes in fission and fusion events, and mitochondrial bioenergetics are important for maintaining neural tissue homeostasis (Van Laar and Barmen, 2013). Involvement of mitochondrial dynamics in neural fate decision is well appreciated during embryonic cortical neurogenesis. Although NSCs in the ventricular zone feature elongated mitochondria, mitochondrial fission dictates progenitor fate in the SVZ and further maturation of neural progenitors to neurons re-exhibits mitochondrial fusion process (Khacho and Slack, 2018; Khacho et al., 2016, 2019; Laaper and Jahani-Asl, 2018). Enhanced mitochondrial fragmentation drives NSCs to neuronal differentiation by mitochondria-to-nuclear retrograde signaling and regulation of nuclear gene expression (Khacho and Slack, 2018; Khacho et al., 2016; Laaper and Jahani-Asl, 2018). Loss of function of mitochondrial fusion or fission proteins has been shown to result in abnormal neuronal development with compromised synapse formation. For instance, mitochondrial fusion protein Mitofusin (MFN2) plays a significant role in neuronal maturation and synapse formation (Fang et al., 2016). Conditional knockout of MFN2 has been shown to result in smaller cerebella and motor deficits (Chen et al., 2007). Similarly, fission protein (DRP1)-deficient mice showed impaired forebrain development (Ishihara et al., 2009). Together, these studies illustrate the importance of mitochondrial dynamics in neuronal development. Despite the growing curiosity to unravel the role of mitochondrial parameters in neural commitment, very little is known about the mitochondrial resident protein SOD2 in neural fate specification.

In the present study we show SOD2 to be essential for early NPC generation, but not for mesoderm or endoderm specification. The neurogenic potential of SOD2 is further established by its ability to override the BMP4-mediated neural inhibition. Attempt to understand the underlying molecular mechanism showed increased mitochondrial fusion by SOD2, mediated by enhanced mitochondrial fusion protein MFN2, but not MFN1. Finally, over-expression of SOD2 along with OCT4 in mouse embryonic fibroblast (MEF) is sufficient to generate induced neural progenitor like cells (iNPLCs), conclusively indicating the neural propensity conferred by SOD2.

RESULTS

SOD2 Expression Is Essential for Neural Fate Specification of mESCs

In our previous study we had reported the role of SOD2 in maintaining STAT3-mediated pluripotency of mouse embryonic stem cells (mESCs) (Sheshadri et al., 2015). In order to understand the role of SOD2 in lineage specification, we analyzed the expression of SOD2 in tri-lineage differentiation of mESCs and found SOD2 to be specifically up-regulated in neural differentiation but not in endo- and mesodermal differentiation of mESCs (Figures 1A and 1B). The observation was further substantiated by the expression of SOD2 in the adult brain tissue of 3-week-old mice (Figure S1A). Directed differentiation of mESCs to neurons and oligodendrocytes showed SOD2 to be specifically detected in neural differentiation, but not in oligodendrocyte differentiation (Figures 1C and S1B), indicating that SOD2 is probably not crucial in other ectodermal sub lineages. Forced expression of SOD2 during neural differentiation demonstrated enhanced expression of neural specific markers—*Pax6, Sox1*, *Zic1* and *Foxg1* at transcript level (Figure 1D) and FOXG1 at protein level (Figure 1E). Addition of BMP4, a potent inhibitor of neural differentiation, to neural induction media reduced the expression of neural genes and *Sod2*S, but forced expression of SOD2 in this condition, induced the expression of early neural markers, suggesting that SOD2 facilitates neural differentiation from mESCs even under non-permissive culture condition (Figure 1F).

To further examine the essentiality of SOD2 in lineage specification and neural induction, we introduced short hairpin RNA (shRNA) specifically targeting SOD2 into mESCs and differentiated them into three derm lineages. Knockdown of SOD2 specifically compromised neural differentiation as evidenced by the down-regulation in the expression of neural lineage markers—*Zic1*, *Sox1* and *Foxg1* (Figure 1G) at transcript and SOX1 at protein levels (Figures 1H and 1I). However, the genes representing the expression of endo- and mesodermal differentiation remained unaltered, suggesting the dispensability of SOD2 in these conditions. To assess whether the effect is specific to SOD2, we tested the role of another SOD family member SOD1 in neural commitment. Neural differentiation of mESCs transduced with *SOD1* shRNA (Figure S2A) showed no reduction in transcript levels of *Pax6*, *Sox1*, and *Nestin* compared with scramble control (Figure S2B). Immunofluorescence for neural marker SOX1 also failed to show any modulation upon *Sod1* shRNA (Figure S2C). We thus ruled out the involvement of SOD1 in mESC neural differentiation. Taken together, these results show that SOD2 is essential for neural commitment of mESCs.

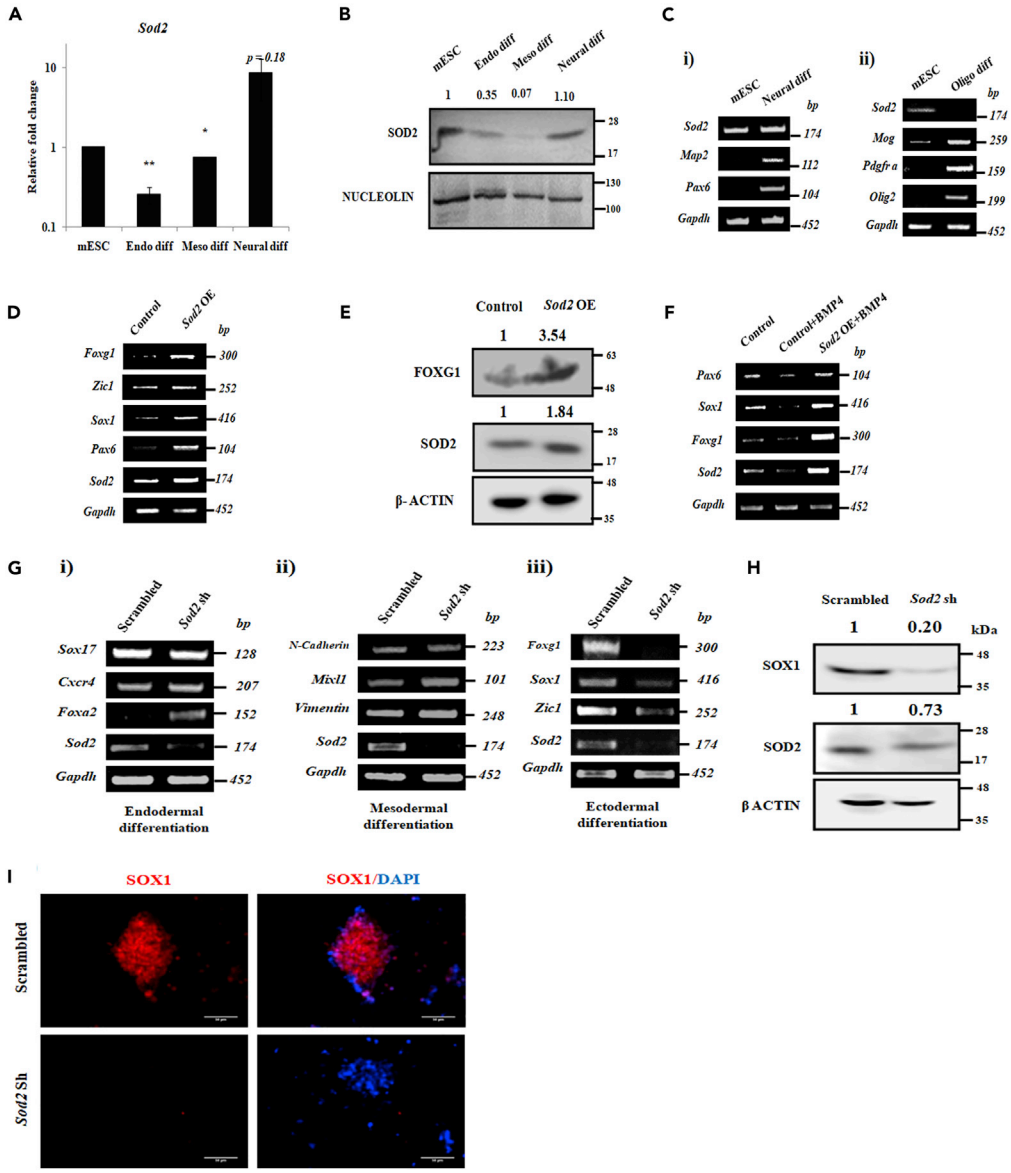

Figure 1. SOD2 Is Essential for the Expression of Neuroectodermal Genes

(A and B) mRNA (A) and protein (B) levels of SOD2 in endoderm, mesoderm, and neural differentiation of mESCs. mRNA levels are plotted as mean ± SE of biological triplicates and statistical significance has been calculated using paired Student's t test, *$p < 0.05$, **$p < 0.01$. (C) mRNA expression of SOD2 and specific markers in neural (i) and oligodendrocyte (ii) differentiation of mESCs. Comparison of mRNA (D) and protein (E) levels of neural markers in SOD2 over-expression against the vector control. (F) Comparison of mRNA levels of neural markers in the vector control, with and without BMP4 treatment, and SOD2 over-expression with BMP4 treatment. (G) Transcript analysis of germ layer markers in endodermal (i), mesodermal (ii), and ectodermal (iii) differentiation from mESCs upon SOD2 knockdown. Expression analysis of early neural marker SOX1 upon SOD2 knockdown in early neural differentiation of mESCs by immunoblotting (H) and immunofluorescence (I). Scale bar represents 50 μm. Un-cropped full western blot images are available in Data S1. List of primers used for transcript analysis and antibodies used for protein detection are available in Tables S1 and S2, respectively.

SOD2 Specifically Modulates Early Neural Differentiation

To ascertain the stage-specific role of SOD2 during neural differentiation, we segregated the differentiation process into two stages—early neural differentiation comprising neural progenitors and late neural differentiation majorly consisting of matured neurons (Figure S1C). During the course of differentiation,

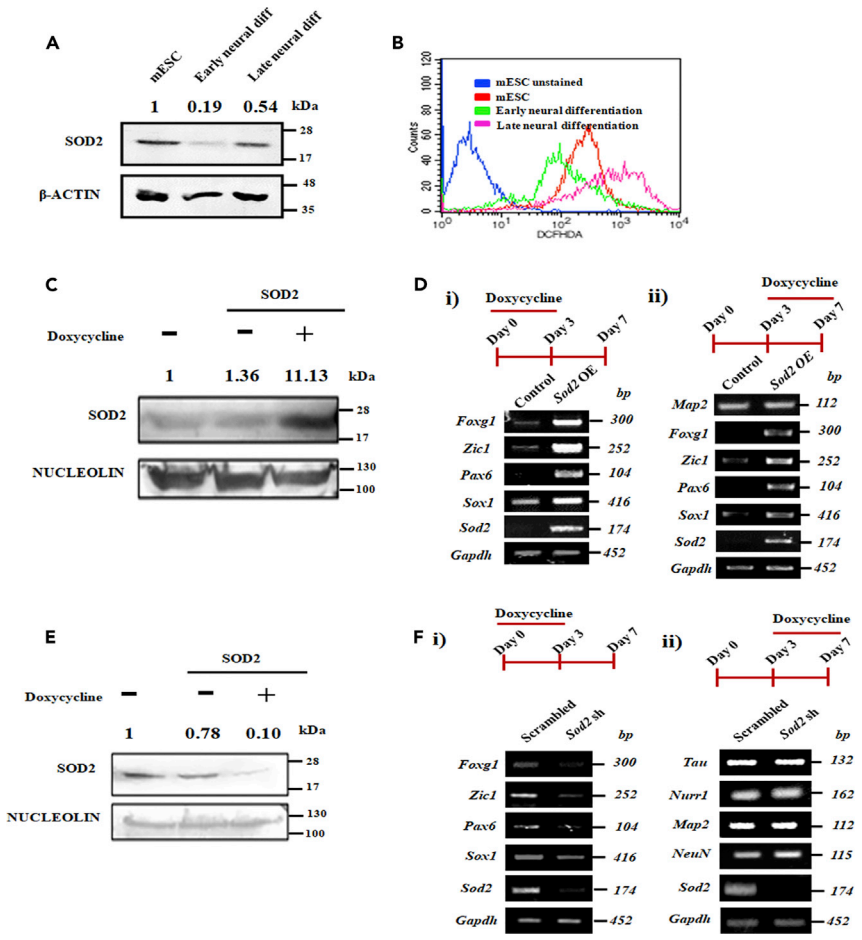

Figure 2. SOD2 Specifically Modulates Early Neural Differentiation

(A) Modulation of protein expression of SOD2 across neural differentiation of mESCs. (B) Analysis of ROS levels using DCFHDA staining during early and late neural differentiation of mESCs. (C) mESCs were transfected with inducible SOD2 over-expression construct and 48 h after addition of doxycycline, cells were harvested and expression of SOD2 analyzed by western blotting. (D) Gene expression analysis of specific neural markers upon SOD2 over-expression induced during (i) early neural differentiation (days 0–3) and (ii) late neural differentiation (days 3–7). (E) mESCs were transfected with inducible SOD2 shRNA construct and 48 h after addition of doxycycline, cells were harvested and expression of SOD2 analyzed by western blotting. (F) Transcript analysis of specific neural markers upon SOD2 knockdown induced during (i) early neural differentiation (days 0–3) and (ii) late neural differentiation (days 3–7). Un-cropped full western blot images are available in data S1. List of primers used for transcript analysis and antibodies used for protein detection are available in Tables S1 and S2, respectively.

biphasic expression pattern of SOD2 was observed wherein lower expression of SOD2 was observed during early neural differentiation compared with mESCs and higher expression during late neural differentiation (Figure 2A). The observed biphasic expression was further supported by a similar trend in superoxide dismutase activity of SOD2 (Figure S1D). Estimation of ROS levels using DCFHDA staining during differentiation showed lower ROS levels in cells of early neural differentiation compared with mESCs and cells of late neural differentiation (Figure 2B), similar to biphasic SOD2 expression. Over-expression of SOD2 using doxycycline-inducible system (Figure 2C) during early neural differentiation showed enhanced expression of early neural markers *Foxg1*, *Zic1*, *Pax6*, and *Sox1* (Figure 2Di), but the over-expression of SOD2 during late neural differentiation resulted in unaltered expression of matured neural marker *Map2* (Figure 2Dii). However, persistent expression of early neural marker was observed even during the late-stage differentiation when doxycycline-induced SOD2 expression was elicited during late-stage neural differentiation (Figure 2Dii). This suggested SOD2 to specifically modulate early neural differentiation. To further probe into the essentiality of SOD2 in the two stages of neural differentiation, we generated inducible shRNA

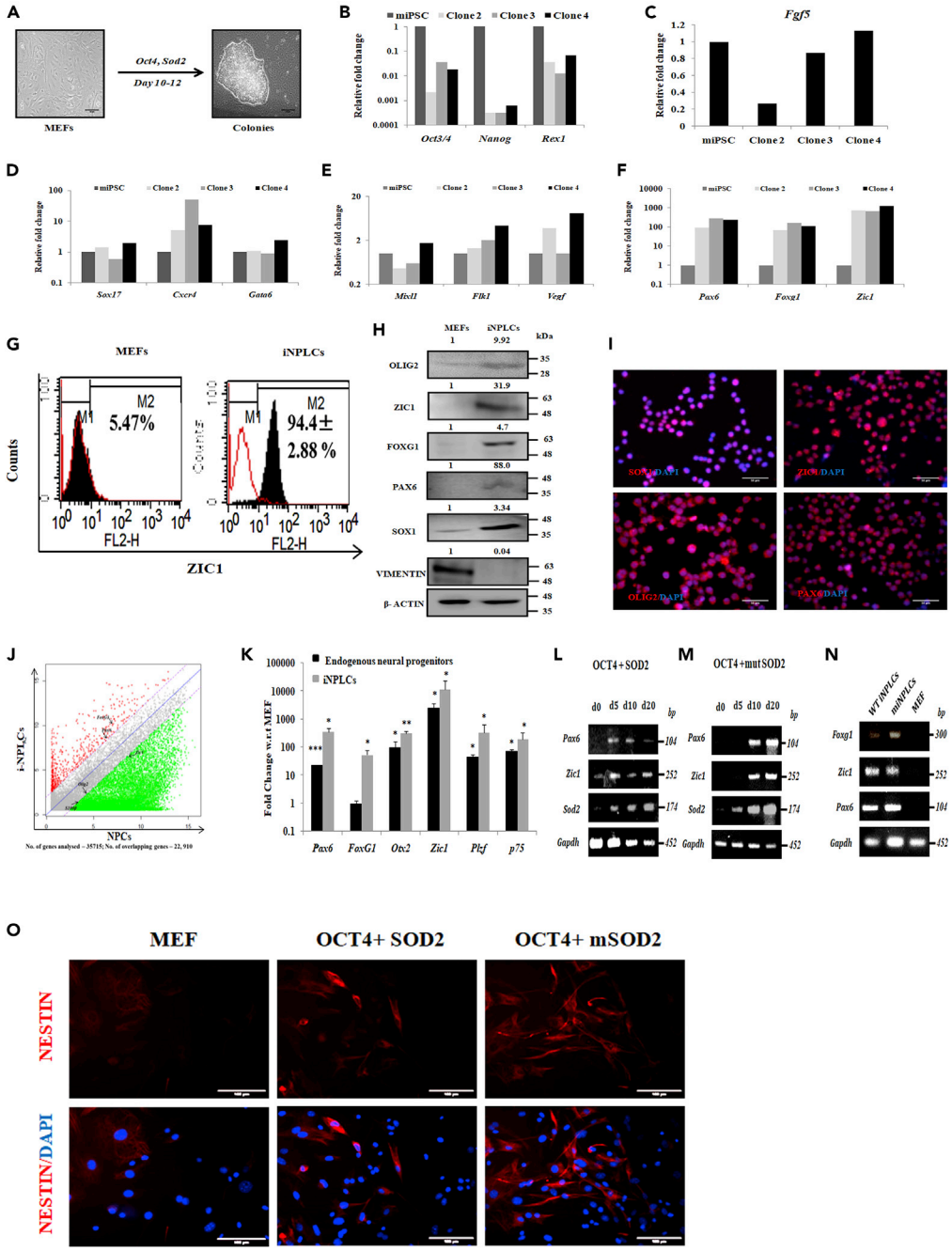

Figure 3. SOD2 along with OCT4 Transdifferentiates MEFs to iNPLCs

(A) Phase contrast images of mouse embryonic fibroblasts (MEF) and colonies obtained from OCT4 and SOD2-mediated transdifferentiation.

(B–K) Characterization of three independent clones obtained by OCT4 and SOD2-transduced cells. Scale bar represents 50 μm. (B) Gene expression analysis of pluripotency markers—*Oct3/4*, *Nanog*, and *Rex1*. (C) Transcript analysis of Epiblast specific marker *Fgf5*. Gene expression analysis of (D) Endodermal markers—*Sox17*, *Cxcr4*, and *Gata6;* (E) Mesodermal markers—*Mixl1*, *Fkl1*, and *Vegf*; and (F) Neural markers—*Pax6*, *Foxg1*, and *Zic1* in iNPLC colonies. (G) Flow cytometric analysis of neural specific marker ZIC1 in MEF and i-NPLCs. (H) Protein levels as analyzed by western blot of early neural markers—ZIC1, SOX1, PAX6, and FOXG1, oligodendrocyte progenitor marker—OLIG2, and fibroblast marker—VIMENTIN in i-NPLCs. (I) Representative immunofluorescence images of neural markers—SOX1, ZIC1, PAX6—and oligodendrocyte progenitor marker—OLIG2—in i-NPLCs. (J) Microarray analysis showing the global gene expression analysis of mouse brain derived neural progenitor cells and i-NPLCs. (K) Comparison of mRNA levels of early neural

Figure 3. *Continued*
markers between endogenous mouse neural progenitors obtained P2 infant brain and i-NPLCs with respect to MEF control.
(L–N) Transcript analysis of neural genes at different time points in MEFs transduced with either Oct4 and WT SOD2 (L) or OCT4 and mutSOD2 (M). Analysis of neural transcripts in cells cultured in NSC medium (N). (O) Immunofluorescence analysis of NESTIN in MEFs transduced with either OCT4 and WT or OCT4 and mutSOD2. Scale bar represents 100 μm. Mean ± SE of biological triplicates, *p < 0.05, **p < 0.01, ***p < 0.001 compared with control MEF. Un-cropped full western blot images are available in data S1. List of primers used for transcript analysis and antibodies used for protein detection are available in Tables S1 and S2, respectively.

and knocked down SOD2 during early and late neural differentiation (Figure 2E) and analyzed the expression of respective neural markers. We found the expression of early neural markers—*Foxg1*, *Zic1*, *Pax6*, and *Sox1*—to be compromised upon SOD2 knockdown during early neural differentiation (Figure 2Fi), but the expression of matured neural markers—*Tau*, *Nurr1*, *Map2* and *NeuN*—remained unchanged upon SOD2 knockdown during late neural differentiation (Figure 2Fii). Altogether, these findings indicate that SOD2 promotes neural differentiation by activating the expression of early neuroectodermal genes.

SOD2 along with OCT4 Is Sufficient to Transdifferentiate MEFs to Neural Progenitor-like Cells

In our previous study we showed a neural transcription factor ZIC3 along with Yamanaka factors to directly transdifferentiate human fibroblast to neural progenitor-like cells (Kumar et al., 2012). Since our results indicated the requirement of SOD2 for neural commitment of mESCs, we wanted to understand whether SOD2 has a similar ability to transdifferentiate MEFs. To address this, we transduced MEFs with various combinations of reprogramming factors OCT4 (O), SOX2 (S), and KLF4 (K) along with SOD2. Except for OSK combination, colonies appeared in all other combinations tested at as early as 12 days (Figure S3A). Interestingly, a minimal combination of OCT4 and SOD2 was sufficient to generate the colonies (Figure 3A), but not individually (data not shown). We continued our further characterization with clones obtained by transducing minimal cocktail of OCT4 and SOD2 transgenes. Expression of endogenous *Oct4* was not detected in these cells, although transgene expression of *Oct4* and *Sod2* was witnessed (Figures S3B and S3C). Lack of fibroblast genes *Col1A1*, *Col3A1*, and *Dkk1* indicated that the cells had indeed lost their fibroblast identity (Figure S3D). Continuing the characterization, we expanded these colonies on feeder-free conditions and performed transcript analysis of the pluripotency markers—*Oct4*, *Sox2*, *Nanog*, and *Rex1*—and found that they lacked the expression of pluripotent genes compared with an established iPSC line (Figure 3B). Also, epiblast specific gene *Fgf5* was not expressed in the colonies (Figure 3C).

Furthermore, to establish the identity of these cells, we performed transcript analysis of tri-lineage specific genes in three individual clones. Although there was minimal expression of endodermal markers (Figure 3D) and mesodermal markers (Figure 3E) in these cells, there was a high expression of neural lineage genes *Pax6, Foxg1*, and *Zic1* (Figure 3F). Flow cytometric analysis for neural specific marker ZIC1 showed that 94.4% of these cells expressed ZIC1 as against 5.47% in MEF (Figure 3G). Immunoblotting revealed expression of neural specific proteins—SOX1, PAX6, FOXG1, and ZIC1—and the oligodendrocyte marker, OLIG2, with a concomitant down-regulation of the fibroblast marker, VIMENTIN (Figure 3H), suggesting the loss of fibroblast memory. Nuclear expression of SOX1, ZIC1, OLIG2, and PAX6 was also observed in these colonies by immunofluorescence (Figure 3I). This suggested that over-expression of OCT4 and SOD2 conferred neural identity to the fibroblast cells and therefore, henceforth these colonies will be designated as induced neural progenitor like cells (iNPLCs). iNPLCs exhibited high morphological homogeneity and could be stably expanded for more than 20 passages without compromise in the expression of neural progenitor genes. With passages, there was decrease in the expression of SOD2 transgene (Figure S3E). In order to determine how similar iNPLCs were to mouse brain derived neural progenitor cells, we performed a global gene expression analysis of iNPLCs and neural progenitor cells (NPCs) derived from P2 mouse brain. Analysis showed that, of 35,715 genes analyzed, expression of 22,910 genes from iNPLCs and P2 mouse NPCs overlapped, accounting for 64% similarity between the two populations (Figure 3J). PCR analysis of a few neural progenitor genes further confirmed a similar expression pattern between iNPLCs and P2 mouse NPCs (Figure 3K). These results show the ability of SOD2 along with OCT4 to transdifferentiate MEFs to iNPLCs.

A hallmark of a bona fide NPLC is its ability to differentiate to matured neurons and glia in *in vitro* and *in vivo* conditions. On providing appropriate cues, iNPLCs could efficiently differentiate to neurons that

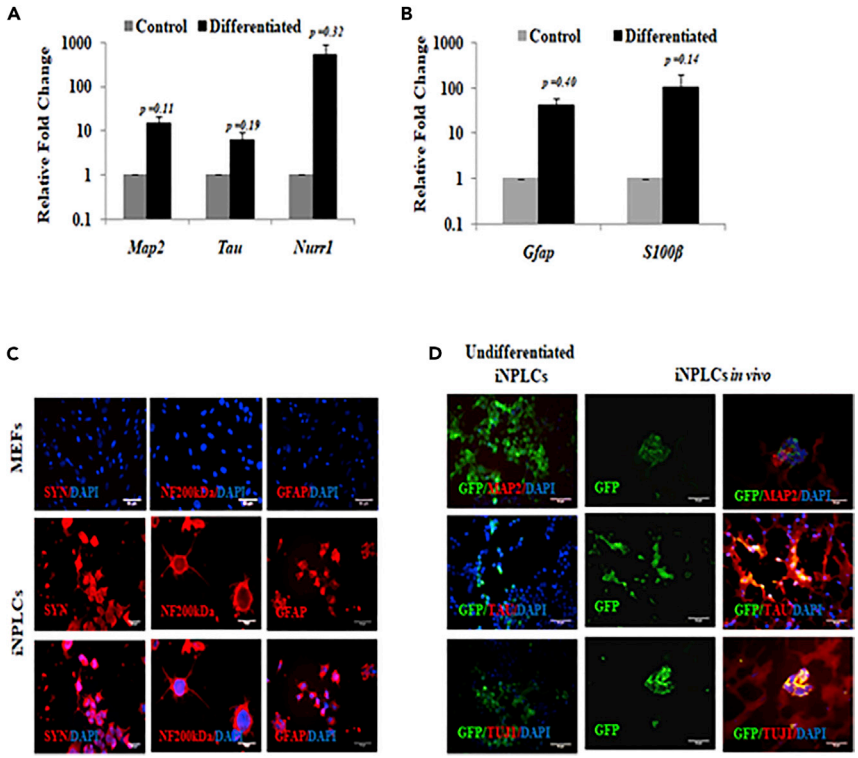

Figure 4. iNPLCs Differentiate to Mature Neurons *In Vitro* and *In Vivo*

(A and B) mRNA levels of matured neural markers (A) and glial markers (B) in iNPLC clones differentiated *in vitro*. (C) Representative immunofluorescence image of matured neuronal and glial markers in iNPLC clones differentiated *in vitro*. (D) Representative immunohistochemistry image showing *in vivo* maturation of injected iNPLC cells harboring GFP plasmid. Mean ± SE, n = 3 independent experiments. Scale bar represents 50 μm. List of primers used for transcript analysis and antibodies used for protein detection are available in Tables S1 and S2, respectively.

expressed *Map2*, *Tau*, and *Nurr1 in vitro* (Figure 4A). Also, in glial differentiation conditions, the cells expressed *Gfap* and *S100β* (Figure 4B). Differentiated iNPLCs also stained positive for matured neural markers—SYNAPTOPHYSIN, NF200kDa—and glial protein—GFAP (Figure 4C). These results validated the *in vitro* differentiation ability of the iNPLCs. Injection of GFP-tagged iNPLCs in the cortex of the neonatal mouse brain and subsequent analysis after 4 weeks showed GFP-positive cells in mouse brain co-expressing matured neural markers MAP2, TAU, TUJ1 (Figure 4D). *In vivo* maturation of iNPLCs thereby conclusively established their neural identity. Thus, the transdifferentiation of MEFs to iNPLCs further reiterated the neurogenic potential of SOD2.

SOD2 Regulates Neurogenesis through Mitochondrial Remodeling

The combined results from mESC differentiation and the transdifferentiation indicate that SOD2 strongly favors the neural lineage over other derm layers during differentiation. To understand the mechanism behind SOD2-mediated neural commitment, we analyzed the conventional role of SOD2 such as altering cell proliferation and quenching of ROS. There was no significant change in cell proliferation upon SOD2 knockdown during neural differentiation as evidenced by Ki67 staining, BrdU incorporation assay, and cell cycle analysis (Figures S4A–S4C). We then speculated that the abrogation of neural differentiation of mESCs upon SOD2 knockdown could be due to increased ROS insult. To resolve this, we knocked down SOD2 and treated the cells with N-acetyl cysteine (NAC), a ROS quencher, during the neural differentiation of mESCs. Gene expression analysis showed no appreciable rescue in the expression of neural markers upon NAC administration in SOD2 knockdown background (Figure S4D). This suggested the dispensability of antioxidant defense in SOD2-mediated neural commitment. In all, these results indicated that the conventional role of SOD2 in regulating cell proliferation and ROS fails to address the mechanism of SOD2-mediated neurogenesis.

As SOD2 is a nuclear-encoded mitochondrial resident enzyme, we sought to observe any modulation in mitochondrial architecture and dynamics as the underlying mechanism. In our initial attempt we transfected MEFs with plasmid encoding DsRed that localizes to mitochondria (mito-DsRed). Fluorescence imaging clearly showed an increase in mitochondrial length upon over-expression of SOD2 (Figure S5A). We quantified the mitochondrial length and categorized them into short: < 0.02 μm; medium: 0.02–0.04 μm; and long: > 0.04 μm. Results clearly indicated an increase in the number of long mitochondria upon SOD2 over-expression, with a concomitant decrease in the short mitochondria (Figure S5B). Quantifying the number of mitochondrial contacts in a time frame showed SOD2 over-expression to increase the number of contacts between mitochondria at 40-, 80-, and 120-s time intervals compared with control (Figure S5C).To further prove this in a cell of neuronal origin, we inhibited SOD2 expression in P40H1, an immortal cell line derived from the hippocampus of a 40-day-old adult immortomouse (Demaegdt et al., 2009) and labeled mitochondria with mito-DsRed. After 72 h of SOD2 inhibition, we observed mitochondria were more fragmented when compared with the scrambled control (Figure 5A). We quantified the length of these mitochondria and found a very significant increase in the number of short mitochondria and a distinct decrease in the number of long mitochondria upon knockdown of SOD2 expression (Figure 5B). On the other hand, ectopic expression of SOD2 showed a significant decrease in the number of short mitochondria and increase in the number of long mitochondria (Figures 5C and 5D). To evaluate the contribution of conventional role of SOD2 in mitochondrial fusion, we generated SOD2 mutant (mutSOD2) constructs wherein the active site residues were mutated to D183N and W185F. Over-expression of mutSOD2 failed to quench the mitochondrial superoxide radicals compared with WT SOD2, as seen by the MitoSox staining (Figure 5E). We further validated the mutSOD2 construct by overexpressing WT and mutSOD2 in the background of SOD2-shRNA that targets the endogenous 3′ UTR and not the overexpressed SOD2 (Figures S6A and S6B). Surprisingly, over-expression of mutSOD2 also enhanced mitochondrial length similar to that of WT wherein significant decrease in the number of short mitochondria and a very significant increase in the number of long mitochondria were observed (Figures 5C and 5D). This observation supported the unconventional role of SOD2—independent of its antioxidant activity—in regulating mitochondrial morphology.

To understand transient fusion events that predict enhanced mitochondrial fusion, we quantified mitochondrial contact events and found that SOD2 over-expression significantly enhanced the transient mitochondrial fusion (~4.5-fold increase in mitochondrial contact compared with control) (Figure 5F, Videos S1 and S2 related to Figure 5). Videos S1 and S2 show the frequency of contacts between mitochondria in control and pMIG SOD2 over-expressing P40H1 cells, respectively. As a direct evidence for mitochondrial fusion, we performed a Venus bio-complementation-based mitochondrial fusion assay where the fusion of mitochondria would lead to Venus fluorescence by the bio-complementation of N terminus (NVZL) and C terminus (CVZL) of Venus localized in two different mitochondria (Figure 5Gi). As a proof of experiment, combined expression of NVZL and CVZL in HEK 293Ts generated venous fluorescence, but not transfected individually (Figure S5D). The specificity of mitochondrial isolation, used for bio-complementation assay, was shown by enrichment of mitochondrial-specific marker COX-6A (Figure S5E). Initial experimental validation in MEF showed increased mitochondrial fusion upon SOD2 expression (Figure S5F). Upon over-expression of SOD2 in neuronal cell line P40H1, we observed a highly significant increase in Venus fluorescence implying enhanced mitochondrial fusion compared with vector alone control (Figure 5Gii). These results suggest that SOD2 positively regulates mitochondrial fusion. These mitochondrial changes upon SOD2 manipulation led us to hypothesize a role for SOD2 in enhancing neural commitment via mitochondrial fusion.

SOD2 Regulates Neurogenesis by MFN2-Mediated Mitochondrial Fusion

Having deciphered the effect of SOD2 on mitochondrial fusion, we wanted to understand the changes in mitochondrial fusion and fission proteins upon SOD2 over-expression. We found up-regulation in the expression of fusion protein MFN2, but no modulation in MFN1 and fission protein FIS1, upon SOD2 over-expression (Figure 6A). This up-regulation of *Mfn2* was evident upon over-expression of WT SOD2 and mutSOD2 at the mRNA and protein levels (Figure S7A and S7C) and SOD2-deficient cells expressed reduced amounts of *Mfn2* (Figure S7B). This led us to hypothesize that MFN2 is an intermediate player in SOD2-mediated neural commitment. To address this, we initially knocked down MFN1 and MFN2 (Figure S7D) individually and simultaneously and looked at the mitochondrial architecture. Mitochondria exhibited fragmentation in each of these conditions compared with the controls, which corroborated the previous results (Chen et al., 2003). Interestingly, SOD2 over-expression rescued the mitochondrial length

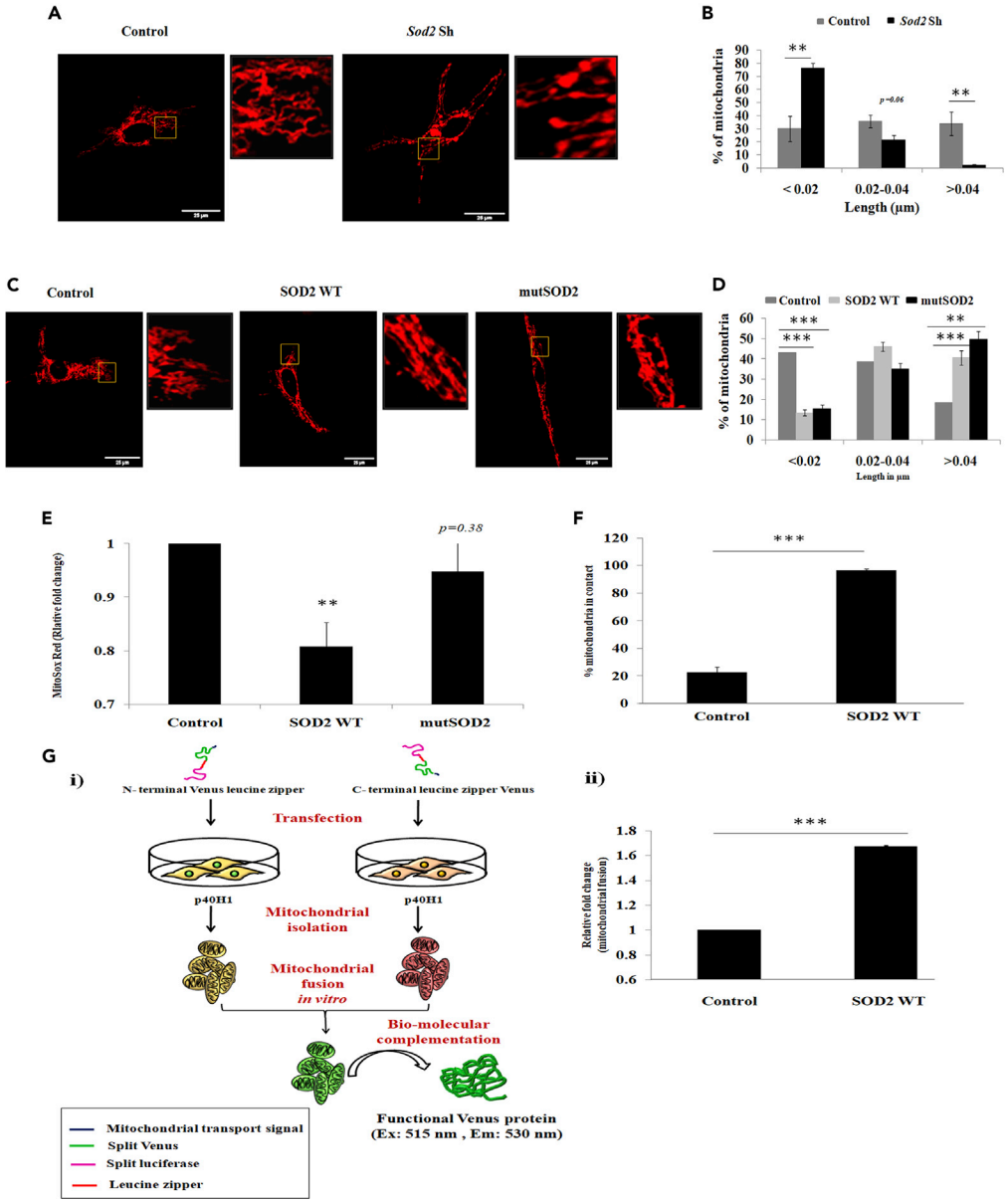

Figure 5. SOD2 Enhances Mitochondrial Fusion Process

(A) Representative confocal images showing modulation in mitochondrial architecture upon SOD2 knockdown in P40H1 cell line. The enlarged image of the boxed region is represented beside each main image. (B) Quantification of mitochondrial length upon SOD2 knockdown in P40H1 cell line. (C) Representative confocal images showing modulation in mitochondrial architecture upon over-expression of wild-type and redox activity mutant constructs of SOD2 in P40H1 cell line. (D) Change in mitochondrial length upon the over-expression of WT and mutant SOD2 in P40H1 cell line. (E) Mitochondrial superoxide levels upon over-expression of SOD2 wild-type and mutant SOD2 constructs as quantified using Mitosox Red staining. (F) Quantification of percentage of mitochondrial contacts upon SOD2 over-expression. (G) (i) Schematic representation depicting the bio-complementation assays used to quantify the mitochondrial fusion process and (ii) the relative fold change in mitochondrial fusion upon SOD2 over-expression as assayed using bio-complementation assay. Data representative of mean ± SE, n = 3 independent experiments, **p < 0.01, ***p < 0.001. Scale bar represents 100 pixels. Twelve images per condition were analyzed and length of ~400 mitochondria was calculated. See also Videos S1 and S2.

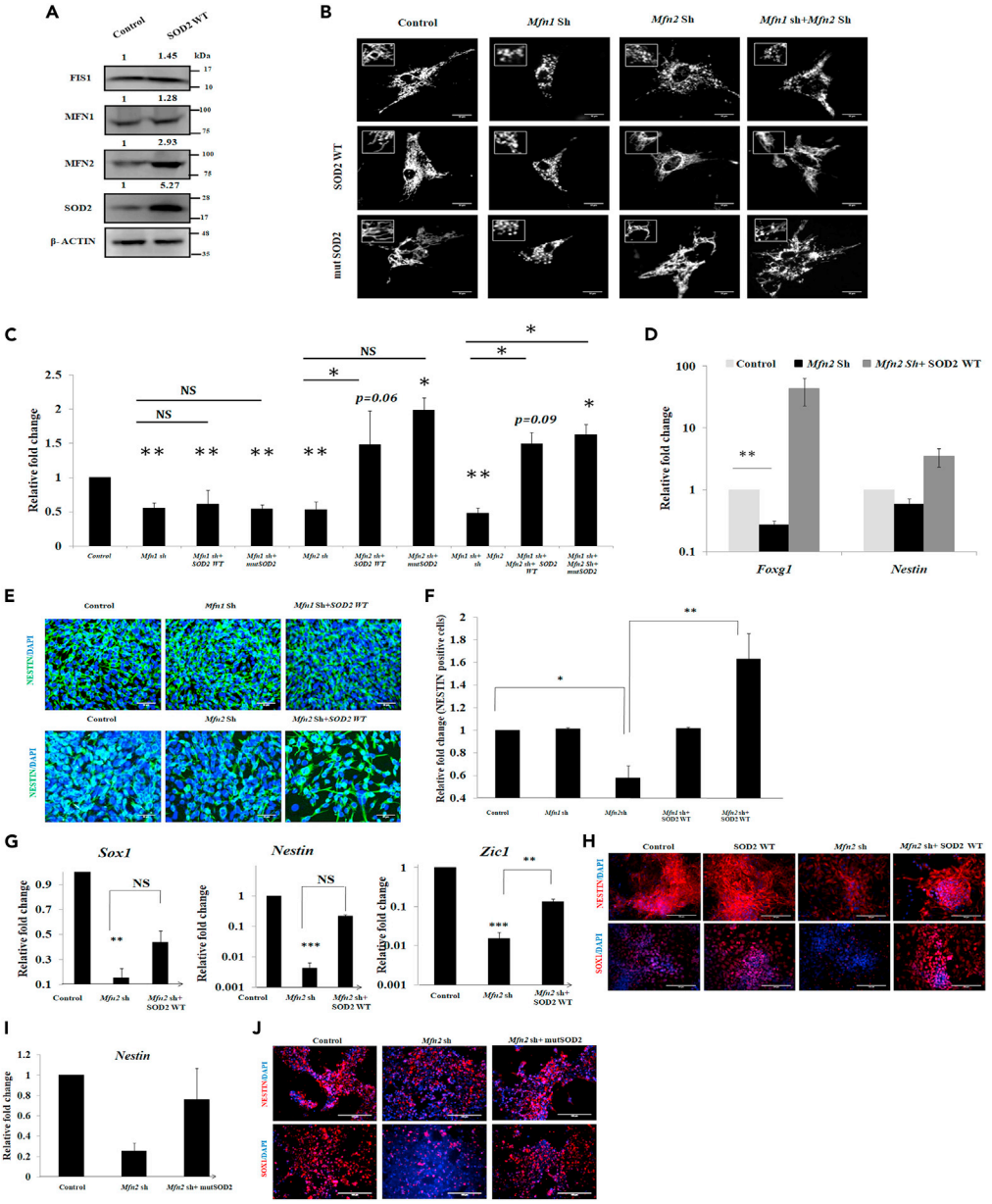

Figure 6. SOD2-Induced Neurogenesis Is by Enhancing Mitochondrial Fusion Process

(A) Protein levels of mitochondrial fission (FIS1) and fusion (MFN1 and MFN2) markers upon SOD2 over-expression. (B) Representative images of mitochondria upon WT or mutSOD2 over-expression in cells where *Mfn1*, *Mfn2*, or both are knocked down. (C) Quantification of mitochondrial length in the conditions as mentioned in the (B). (D) mRNA levels of early neural markers (*Foxg1 and Nestin*) in P40H1 cells with conditions wherein *SOD2* is over-expressed in cells with *Mfn2* knockdown. (E) Representative immunofluorescence images of NESTIN in neural cells with *Mfn 1*, *Mfn 2* individual or simultaneous knockdown and subsequent *SOD2* over-expression. Scale bar represents 50 μm. (F) Relative fold change in the percentage of NESTIN-positive cells upon knockdown of *Mfn 1*, *Mfn2*, or both, and subsequent *SOD2* over-expression. (G) Transcript analysis showing rescue in neural markers *Sox1*, *Nestin*, and *Zic1* of mESCs differentiated to neural progenitors under *Mfn2* shRNA and over-expression of SOD2 conditions. (H) Immunofluorescence images of NESTIN and SOX1 showing rescue in neural differentiation upon over-expression of SOD2 in *Mfn2* knockdown background. (I) Transcript analysis of *Nestin* and (J) immunofluorescence for NESTIN and SOX1 showing rescue in neural differentiation of mESCs upon over-expression of antioxidant activity mutant SOD2 under *Mfn2* shRNA condition. Scale bar represents 100 μm. Data representative of mean ± SE, n = 3 independent experiments, *p < 0.05, **p < 0.01, ***p < 0.001. Number of mitochondria counted per condition ~400. Un-cropped full western blot images are available in data S1. List of primers used for transcript analysis and antibodies used for protein detection are available in Tables S1 and S2, respectively.

when MFN2 was inhibited individually or together with MFN1. However, the rescue in mitochondrial length upon SOD2 over-expression was not observed when MFN1 alone was knocked down. These results suggested that SOD2 exerts its effect on mitochondrial fusion by regulating MFN2 specifically and not MFN1 (Figure 6B). To further determine whether the antioxidant activity of SOD2 is required for MFN2-mediated fusion process, WT and mutSOD2 were over-expressed in cells where MFN2 is either inhibited individually or combined with MFN1. Surprisingly, similar to SOD2 WT, we found mutSOD2 to rescue the mitochondrial length only in those cells where MFN2 was inhibited but not in the cells where MFN1 was knocked down (Figure 6B). The observation was further supported by the quantitative assessment of mitochondrial length using mito DsRed transfected images under all the genetic manipulation conditions in P40H1 cells (Figure 6C). These results demonstrated the dispensability of the antioxidant activity of SOD2 in mitochondrial fusion process. To validate this observation, we sought after transdifferentiation approach wherein we overexpressed mutSOD2 along with OCT4 to transdifferentiate MEFs. Post over-expression, we observed generation of colonies resembling those generated with WT SOD2 (Figure S3F). Upon transcript analysis, cells overexpressing mutSOD2 and OCT4 showed expression of neural markers *Pax6*, *Foxg1*, and *Zic1* similar to those transduced with OCT4 and WT SOD2 (Figures 3L and 3M). Culturing these cells in NSC medium further induced neural signatures that were undetected in MEF control (Figure 3N). Transduction of SOD2 WT and mutSOD2 individually along with OCT4 resulted in generation of NESTIN-positive cells, thus confirming their NPLC identity (Figure 3O) and thus reiterated the antioxidant activity of SOD2 to be trivial in regulating neural commitment.

To convincingly demonstrate that the role of SOD2 in neurogenesis is via specific modulation of MFN2 expression, we analyzed the expression of neural genes in P40H1 over-expressing SOD2 in MFN1/MFN2 knockdown conditions. There was no detectable change in the expression of neural marker NESTIN in the conditions where either MFN1 was knocked down or SOD2 over-expressed in MFN1 knockdown condition. On the other hand, there was a clear decrease in the expression of *Foxg1* and *Nestin* at the transcript level (Figure 6D) and number of NESTIN-positive cells upon MFN2 knockdown, which was significantly rescued upon over-expression of SOD2 (Figures 6E and 6F). To authenticate the observation, we choose an independent model system of differentiating mESCs to NPCs. Similar inhibition of MFN2 during differentiation of mESCs to NPCs led to compromised expression of neural progenitor markers *Sox1*, *Nestin*, and *Zic1* (Figure 6G) at the transcript level and SOX1 and NESTIN at the protein level (Figure 6H). Over-expression of SOD2 in MFN2 knockdown background led to rescue in the expression of these markers similar to the controls (Figures 6G and 6H). To test whether the SOD's antioxidant activity is required for the rescue in the expression of these genes, we over-expressed mutSOD2 in place of WT SOD2 in cells lacking MFN2 expression and observed a similar rescue in the transcript level of *Nestin* (Figure 6I) and SOX1 and NESTIN at the protein level to that of WT SOD2 (Figure 6J). These results implicate a potential role for SOD2 in neurogenesis by modulating the mitochondrial length and dynamics via the regulation of MFN2, independent of its antioxidant activity.

DISCUSSION

Mitochondrial resident SOD2 is traditionally viewed as an enzyme involved in dismutation of superoxide anion to hydrogen peroxide. The role played by SOD2 beyond its antioxidant activity, especially in terms of derm layer specification during development, remains largely unexplored. In 2012, Hou et al. reported that SOD2 knockout mice have significantly lesser proliferating NPCs compared with WT. This difference was attributed to increased superoxide flashes, in cells lacking SOD2, ultimately resulting in abrogation of neural progenitors in embryonic mouse cortex (Hou et al., 2012). It has also been shown that increased expression of SOD2 attenuates apoptosis of mesodermal cardiomyocytes and ameliorates myocardial infarction (Long et al., 2017). Despite these initial clues, a comprehensive understanding of SOD2's involvement in lineage specification remained elusive.

Previous studies from our laboratory and others had elucidated the role of SOD2 in maintaining stem cell pluripotency (Sheshadri et al., 2015; Solari et al., 2015). Following this observation, we expected that its inhibition would enhance tri-lineage differentiation of mESCs. However, upon knockdown of SOD2, mESCs failed to acquire neural fate without impeding the expression of meso- and endoderm lineage genes. These observations are well corroborated with previous *in vivo* studies wherein mice lacking SOD2 specifically in brain, but not other antioxidant enzymes, showed perinatal death and exhibited spongiform neurodegeneration in motor cortex, hippocampus, and brainstem (Izuo et al., 2015). Surprisingly, although knockdown and over-expression of SOD2 during differentiation of mESCs showed a modulation in neural

differentiation at early stage, the results from normal differentiation condition showed a reduction in SOD2 during early stage of differentiation in contrast to anticipated up-regulation. The probable reason for this conflicting observation is that, as SOD2 is also involved in maintenance of pluripotency of mESCs, down-regulation of SOD2 is necessary to exit from the pluripotent state to get differentiated. Therefore, a critical level of SOD2 is essential for conferring neural fate and expressing SOD2 over and above this level resulted in persistent maintenance of enhanced expression of neural progenitor genes during maturation with concomitant decrease in matured genes. So, during normal neural differentiation decreased expression of SOD2 is probably implemented to favor the transition of NPCs to matured neurons. To test the neurogenic potential of SOD2, we sought a more stringent approach, i.e., transdifferentiation, using SOD2. In the present study, a minimal cocktail of SOD2 and OCT4 was sufficient to transdifferentiate MEF to iNPLC, advocating the neurogenic potential of SOD2. As reported earlier, the probable role of OCT4 in this cocktail is to shape chromatin accessibility and pave way for other transcription factors to bind to its promoter (King and Klose, 2017). Further differentiation of these cells to neurons *in vitro* and *in vivo* conclusively established the ability of SOD2 to confer neural identity to terminally differentiated MEFs. These observations conclusively advocated a pivotal role for SOD2 in conferring neural proclivity.

Having convincingly precluded cell proliferation and antioxidant defense as plausible mechanisms, we contemplated on modulation in mitochondrial architecture and dynamics as an alternative mechanism underlying SOD2-mediated neural differentiation. Liu et al., demonstrated that, by increasing the mitochondrial membrane potential, transdifferentiation of human dermal stem cells to functional neurons could be achieved (Liu et al., 2019). Previous studies also reported mitochondrial dynamics established through regulated fission and fusion to dictate the fate decisions of neural stem cells (Khacho and Slack, 2018; Khacho et al., 2016, 2019). These observations compelled us to investigate the role of mitochondrial dynamics as a probable mechanism underlying SOD2-mediated neurogenesis. An independent report by Zhao et al. showed SOD2 to increase neurite growth in primary cortical neurons by decreasing fission protein DRP1R and in turn reducing mitochondrial fragmentation (Zhao et al., 2019). However, in our present study, by multiple approaches, we found that SOD2 enhances mitochondrial fusion by specifically up-regulating MFN2, but not MFN1. Probably, this up-regulation of MFN2 might be a chosen mechanism to favor neurogenesis by SOD2.

MFN2 is a mitochondrial outer membrane protein that mediates outer mitochondrial membrane (OMM) fusion. Several studies have shown the importance of MFN2 in neuronal maturation (Fang et al., 2016), cerebellar development (Chen et al., 2007), and synapse formation (Fang et al., 2016). Studies by Pham et al. showed specific loss of *Mfn2*, but not *Mfn1*, to impair dopaminergic neuron function and result in motor deficit (Pham et al., 2012). Compared with *Mfn2*, levels of *Mfn1* are very low in the nervous system. Probably owing to this, conditional knockout of *Mfn2*, but not Mfn1, results specifically in neurodegeneration. In our study also, we observed knockdown of *Mfn2*, but not *Mfn1*, to result in reduced neural gene expression. Also, in corroboration with previous reports, knockdown of either *Mfn1* or *Mfn2* resulted in mitochondrial fragmentation, but SOD2 had the ability to rescue mitochondrial fragmentation only in *Mfn2* knockdown condition, reiterating SOD2 to specifically regulate *Mfn2*-mediated effects and this turns out to be one of the underlying mechanisms in SOD2-mediated neurogenesis. However, our attempts to understand how SOD2 influences the MFN2 activity neither showed SOD2's physical interaction with MFN2 and modulation of its fusion activity nor did it prevent MFN2 from undergoing protein degradation (data not shown).

In conclusion, our work defines an important antioxidant-independent role for SOD2 in specifically up-regulating the fusion protein MFN2 and promoting neural specification. This property of SOD2 has assisted in generating a novel cocktail for transdifferentiating mouse fibroblasts to iNPLCs. Collectively, our work provides a new functional implication for SOD2 in neural lineage specification.

Limitations of the Study

Our study reveals a crucial role of SOD2 in the regulation of early neural fate commitment using different model systems. We also show the ability of SOD2 to switch the fate of MEFs to neural progenitor-like cells *in vitro*. And these were independent of antioxidant activity of SOD2. Along the process we found SOD2 to influence mitochondrial dynamics where in it facilitates fusion process by up-regulating MFN2. A major limitation of the study is that the mechanism by which SOD2 regulates MFN2 expression remains elusive. We attempted to understand the relation between SOD2 and MFN2 by performing co-immunoprecipitation experiments. The results indicated the absence of any interaction between SOD2 and MFNs. As an

alternative, we carried out experiments to see if SOD2 shielded MFNs from undergoing degradation. Although MFNs were degraded with time in presence of Cycloheximide, their stability was not maintained even under SOD2 over-expression. Despite attempts, the study leaves behind an unanswered query of mechanism underlying SOD2-mediated up-regulation of MFN2.

Resource Availability

Lead Contact

Further information and requests for resources and reagents should be directed to and will be fulfilled by the lead contact, Anujith Kumar: anujith.kumar@manipal.edu.

Materials Availability

All the in-house generated plasmid constructs as mentioned in Table S2, Transparent Methods supplemental file, are available upon request.

Data and Code Availability

The data that support the findings of this study are available from the Lead Contact on reasonable request. Microarray data have been deposited in Gene Expression Omnibus (GEO) and are accessible through GEO series accession number GSE154756.

METHODS

All methods can be found in the accompanying Transparent Methods supplemental file.

SUPPLEMENTAL INFORMATION

Supplemental Information can be found online at https://doi.org/10.1016/j.isci.2020.101564.

ACKNOWLEDGMENTS

This study was supported by grants from Department of Biotechnology, India (BT/PR 6165/GBD/27/369/2012, BT/PR8508/MED/30/1019/2013 and BT/PR15508/MED/31/316/2015) to A.K. We thank Prof. Panicker for kindly providing the cell line P40H1. We thank Prof. Heidi Mcbride for the plasmids C-mito LZV and N-mito VZL. pLV-mitoDsRed was a gift from Pantelis Tsoulfas (Addgene plasmid #44386). We thank Central Imaging and Flow Cytometry Facility, National Center for Biological Sciences, Bangalore, for helping in confocal imaging.

AUTHOR CONTRIBUTIONS

Conceptualization, S.B., P.S., J.P., and A.K.; Methodology and Formal Analysis, S.B., P.S., and A.K.; Investigation, S.B., P.S., J.P.J., and C.P.; Writing – Original Draft, S.B., J.P.J., and A.K.; Writing – Review & Editing: S.B., P.S., J.P., and A.K.; Supervision, A.K.; Funding Acquisition, A.K.

DECLARATION OF INTERESTS

The authors declare no competing interest.

Received: December 3, 2019
Revised: July 28, 2020
Accepted: September 11, 2020
Published: October 23, 2020

REFERENCES

Agostini, M., Romeo, F., Inoue, S., Niklison-Chirou, M.V., Elia, A.J., Dinsdale, D., Morone, N., Knight, R.A., Mak, T.W., and Melino, G. (2016). Metabolic reprogramming during neuronal differentiation. Cell Death Differ. *23*, 1502–1514.

Alvarez-buylla, A., and Garcı, J.M. (2002). Neurogenesis in adult subventricular zone. J. Neurosci. *22*, 629–634.

Arrázola, M.S., Andraini, T., Szelechowski, M., Mouledous, L., Arnauné-Pelloquin, L., Davezac, N., Belenguer, P., Rampon, C., and Miquel, M.C. (2019). Mitochondria in developmental and adult neurogenesis. Neurotox. Res. *36*, 257–267.

Beckervordersandforth, R., Ebert, B., Schäffner, I., Moss, J., Fiebig, C., Shin, J., Moore, D.L., Ghosh, L., Trinchero, M.F., Stockburger, C., et al. (2017). Role of mitochondrial metabolism in the control of early lineage progression and aging phenotypes in adult hippocampal neurogenesis. Neuron *93*, 560–573.e6.

Bond, A.M., Ming, G., and Song, H. (2015). Adult mammalian neural stem cells and neurogenesis: Five Decades Later. Cell Stem Cell *17*, 385–395.

Chen, H., Detmer, S.A., Ewald, A.J., Griffin, E.E., Fraser, S.E., and Chan, D.C. (2003). Mitofusins Mfn1 and Mfn2 co-ordinately regulate mitochondrial fusion and are essential for embryonic development. J. Cell Biol. *160*, 189–200.

Chen, H., McCaffery, J.M., and Chan, D.C. (2007). Mitochondrial fusion protects against neurodegeneration in the cerebellum. Cell *130*, 548–562.

Cheng, A., Yang, Y., Zhou, Y., Maharana, C., Lu, D., Peng, W., Liu, Y., Wan, R., Marosi, K., Misiak, M., et al. (2016). Mitochondrial SIRT3 mediates adaptive responses to neurons to exercise and metabolic and excitatory challenges. Cell Metabol. *23*, 128–142.

Demaegdt, H., Lukaszuk, A., De Buyser, E., De Backer, J.P., Szemenyei, E., Tóth, G., Chakravarthy, S., Panicker, M., Michotte, Y., Tourwé, D., and Vauquelin, G. (2009). Selective labeling of IRAP by the tritiated AT4 receptor ligand [3H] Angiotensin IV and its stable analog [3H] AL-11. Mol. Cell Endocrinol. *13*, 77–86.

Eriksson, P.S., Perfilieva, E., Bjork- Eriksson, T., Alborn, A.M., Nordborg, C., Peterson, D.A., and Gage, F.H. (1998). Neurogenesis in the adult human hippocampus. Nat. Med. *4*, 1313.

Fang, D., Yan, S., Yu, Q., Chen, D., and Yan, S.S. (2016). Mfn2 is required for mitochondrial development and synapse formation in human induced pluripotent stem cells/hiPSC derived cortical neurons. Sci. Rep. *6*, 31462.

Hou, Y., Ouyang, X., Wan, R., Cheng, H., Mattson, M.P., and Cheng, A. (2012). Mitochondrial superoxide production negatively regulates neural progenitor proliferation and cerebral cortical development. Stem Cells *30*, 2535–2547.

Izuo, N., Nojiri, H., Uchiyama, S., Noda, Y., Kawakami, S., Kojima, S., Sasaki, T., Shirasawa, T., and Shimizu, T. (2015). Brain-specific superoxide dismutase 2 deficiency causes perinatal death with spongiform encephalopathy in mice. Oxid. Med. Cell. Longev. *2015*, 1–10.

Ishihara, N., Nomura, M., Jofuku, A., Kato, H., Suzuki, S.O., Masuda, K., and Taguchi, N. (2009). Mitochondrial fission factor Drp1 is essential for embryonic development and synapse formation in mice. Nat. Cell. Biol. *11*, 958.

Khacho, M., and Slack, R.S. (2018). Mitochondrial dynamics in the regulation of neurogenesis: from development to the adult brain. Dev. Dyn. *247*, 47–53.

Khacho, M., Clark, A., Svoboda, D.S., Harper, M., Park, D.S., and Slack, R.S. (2016). Mitochondrial dynamics impacts stem cell identity and fate decisions by regulating a nuclear transcriptional program. Cell Stem Cell *19*, 1–16.

Khacho, M., Harris, R., and Slack, R.S. (2019). Mitochondria as central regulators of neural stem cell fate and cognitive function. Nat. Rev. Neurosci. *20*, 34–48.

King, H.W., and Klose, R.J. (2017). The pioneer factor OCT4 requires the chromatin remodeller BRG1 to support gene regulatory element function in mouse embryonic stem cells. Elife *6*, 1–24.

Klivenyi, P., St. Clair, D., Wermer, M., Yen, H.C., Oberley, T., Yang, L., and Beal, M.F. (1998). Manganese superoxide dismutase overexpression attenuates MPTP toxicity. Neurobiol. Dis. *5*, 253–258.

Kumar, A., Declercq, J., Eggermont, K., Agirre, X., Prosper, F., and Verfaille, C.M. (2012). Zic3 induces conversion of human fibroblasts to stable neural progenitor- like cells. J. Mol. Cell Biol. *4*, 252–255.

Laaper, M., and Jahani-Asl, A. (2018). Regulation of neural stem cell fate decisions by mitochondrial dynamics. Neural Regen. Res. *13*, 1548–1549.

Liu, H., He, Z., April, S.L., Trefny, M.P., Rougier, J.S., Salemi, S., Olariu, R., Widmer, H.R., and Simon, H.U. (2019). Biochemical re-programming of human dermal stem cells to neurons by increasing mitochondrial membrane potential. Cell Death Differ. *26*, 1048–1061.

Long, B., Gan, T.Y., Zhang, R.C., and Zhang, Y.H. (2017). miR-23a regulates cardiomyocyte apoptosis by targeting manganese superoxide dismutase. Mol. Cell *40*, 542–549.

Martynoga, B., Drechsel, D., and Guillemot, F. (2012). Molecular control of neurogenesis: a view from the mammalian cerebral cortex. Cold Spring Harb. Perspect. Biol. *4*, a008359.

Massaad, C.A., Washington, T.M., Pautler, R.G., and Klann, E. (2009). Overexpression of SOD-2 reduces hippocampal superoxide and prevents memory deficits in a mouse model of Alzheimer's disease. Proc. Natl. Acad. Sci. U S A *106*, 13576–13581.

Oh, S.S., Sullivan, K.A., Wilkinson, J.E., Backus, C., Hayes, J.M., Sakowski, S.A., and Feldman, E.L. (2012). Neurodegeneration and early lethality in superoxide dismutase 2-deficient mice: a comprehensive analysis of the central and peripheral nervous systems. Neuroscience *212*, 201–213.

Pham, A.H., Meng, S., Chu, Q.N., and Chan, D.C. (2012). Loss of Mfn2 results in progressive, retrograde degeneration of dopaminergic neurons in the nigrostriatal circuit. Hum. Mol. Genet. *21*, 4817–4826.

Sheshadri, P., Ashwini, A., Jahnavi, S., Bhonde, R., Prasanna, J., and Kumar, A. (2015). Novel role of mitochondrial manganese superoxide dismutase in STAT3 dependent pluripotency of mouse embryonic stem cells. Sci. Rep. *5*, 1–12.

Solari, C., Echegaray, C.V., Cosentino, M.S., Petrone, M.V., Waisman, A., Luzzani, C., Francia, M., Villodre, E., Lenz, G., Miriuka, S., et al. (2015). Manganese superoxide dismutase gene expression is induced by Nanog and Oct4, essential pluripotent stem cells' transcription factors. PLoS One *10*, 1–12.

Stiles, J., and Jernigan, T.L. (2010). The basics of brain development. Neuropsychol. Rev. *20*, 327–348.

Toni, N., Teng, E.M., Bushong, E.A., Aimone, J.B., Zhao, C., Consiglio, A., Van Praag, H., Martone, M.E., Ellisman, M.H., and Gage, F.H. (2007). Synapse formation on neurons born in the adult hippocampus. Nat. Neurosci. *10*, 727–734.

Turrens, J.F. (2003). Mitochondrial formation of reactive oxygen species. J. Physiol. *552*, 335–344.

Van Laar, V.S., and Berman, S.B. (2013). The interplay of neuronal mitochondrial dynamics and bioenergetics: implications for Parkinson's disease. Neurobiol. Dis. *51*, 43–55.

Wang, Y., Branicky, R., Noë, A., and Hekimi, S. (2018). Superoxide dismutases: Dual roles in controlling ROS damage and regulating ROS signaling. J. Cell Biol. *217*, 1915–1928.

Yon, J.M., Baek, I.J., Lee, B.J., Yun, Y.W., and Nam, S.Y. (2011). Dynamic expression of manganese superoxide dismutase during mouse embryonic organogenesis. Int. J. Dev. Biol. *55*, 327–334.

Zhao, Q., Lu, D., Wang, J., Liu, B., Cheng, H., Mattson, M.P., and Cheng, A. (2019). Calcium dysregulation mediates mitochondrial and neurite outgrowth abnormalities in SOD2 deficient embryonic cerebral cortical neurons. Cell Death Differ. *26*, 1600–1614.

iScience, Volume *23*

Supplemental Information

Mitochondrial Superoxide Dismutase Specifies Early Neural Commitment by Modulating Mitochondrial Dynamics

Smitha Bhaskar, Preethi Sheshadri, Joel P. Joseph, Chandrakanta Potdar, Jyothi Prasanna, and Anujith Kumar

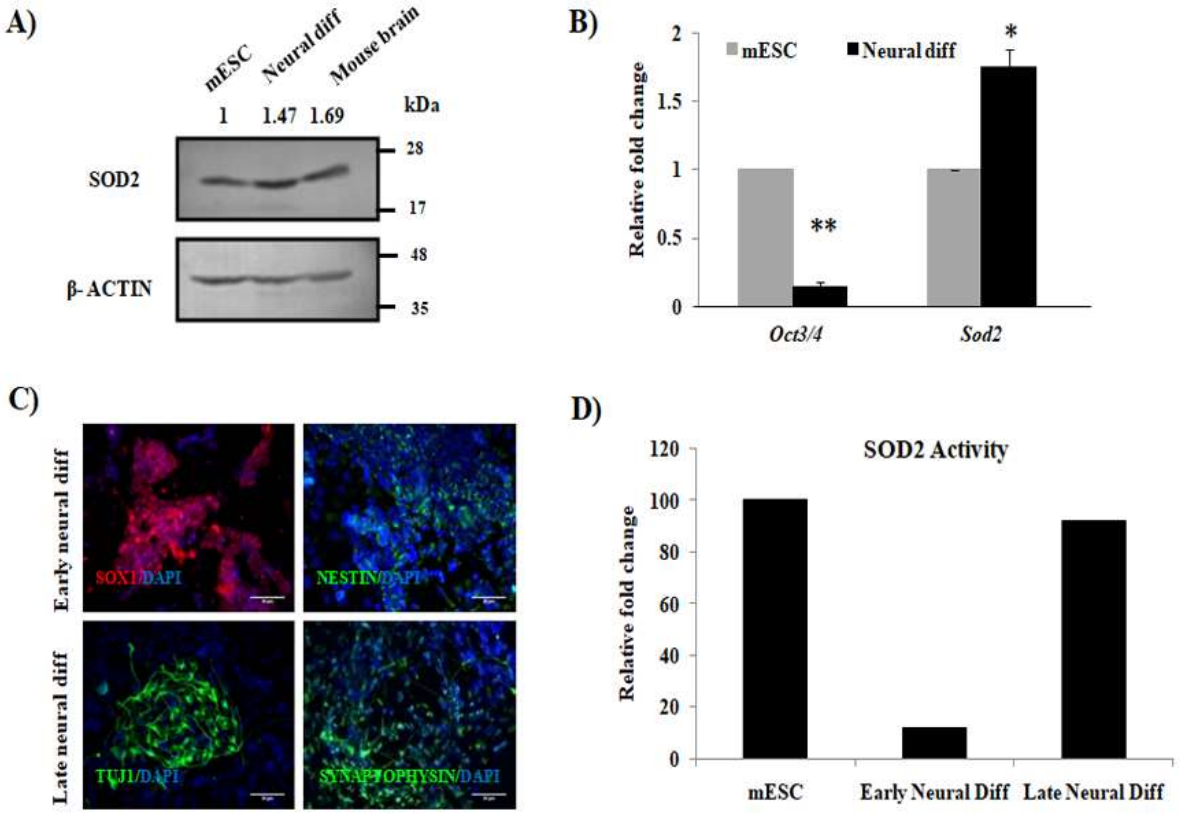

Figure S1, related to figure 1: Expression and enzymatic activity analysis of SOD2 during neural differentiation of mESCs.

(A) Protein levels of SOD2 in mESCs, neural differentiation and adult brain tissue.

(B) mRNA levels of *Oct3/4* and *Sod2* in mESCs and its neural differentiation counterpart.

(C) Representative immunofluorescence images to authenticate the early (SOX1, NESTIN) and late (TUJ1, SYNAPTOPHYSIN) neural differentiation stages of cells differentiated from mESCs.

(D) Fold change in SOD2 enzyme activity in early neural differentiation and late neural differentiation in comparison with mESCs. Mean ±SE, n= 3 independent experiments, * $p< 0.05$, ** $p < 0.01$.

Un-cropped full western blot images are available in data S1.

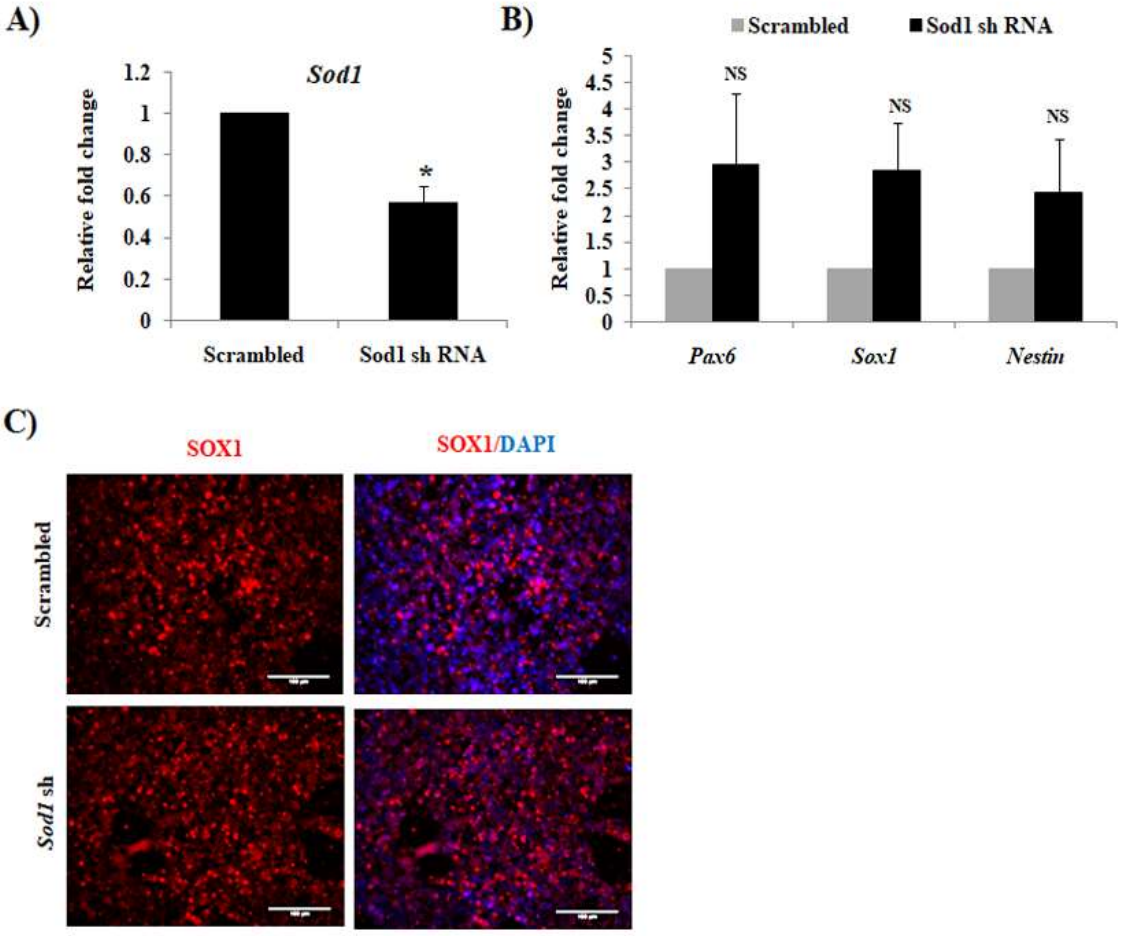

Figure S2, related to figure 1: Effect of Sod1 knockdown on neural differentiation of mESCs.

A) Knock-down efficiency of *Sod1* shRNA in mESCs.

B) Transcript analysis showing effect of *Sod1* knockdown on neural differentiation of mESCs.

C) Immunofluorescence for SOX1 in neural differentiation of mESCs upon *Sod1*inhibition. Data represented as mean ±SE, n= 3 independent experiment, *p< 0.05. Scale bar= 100 µm.

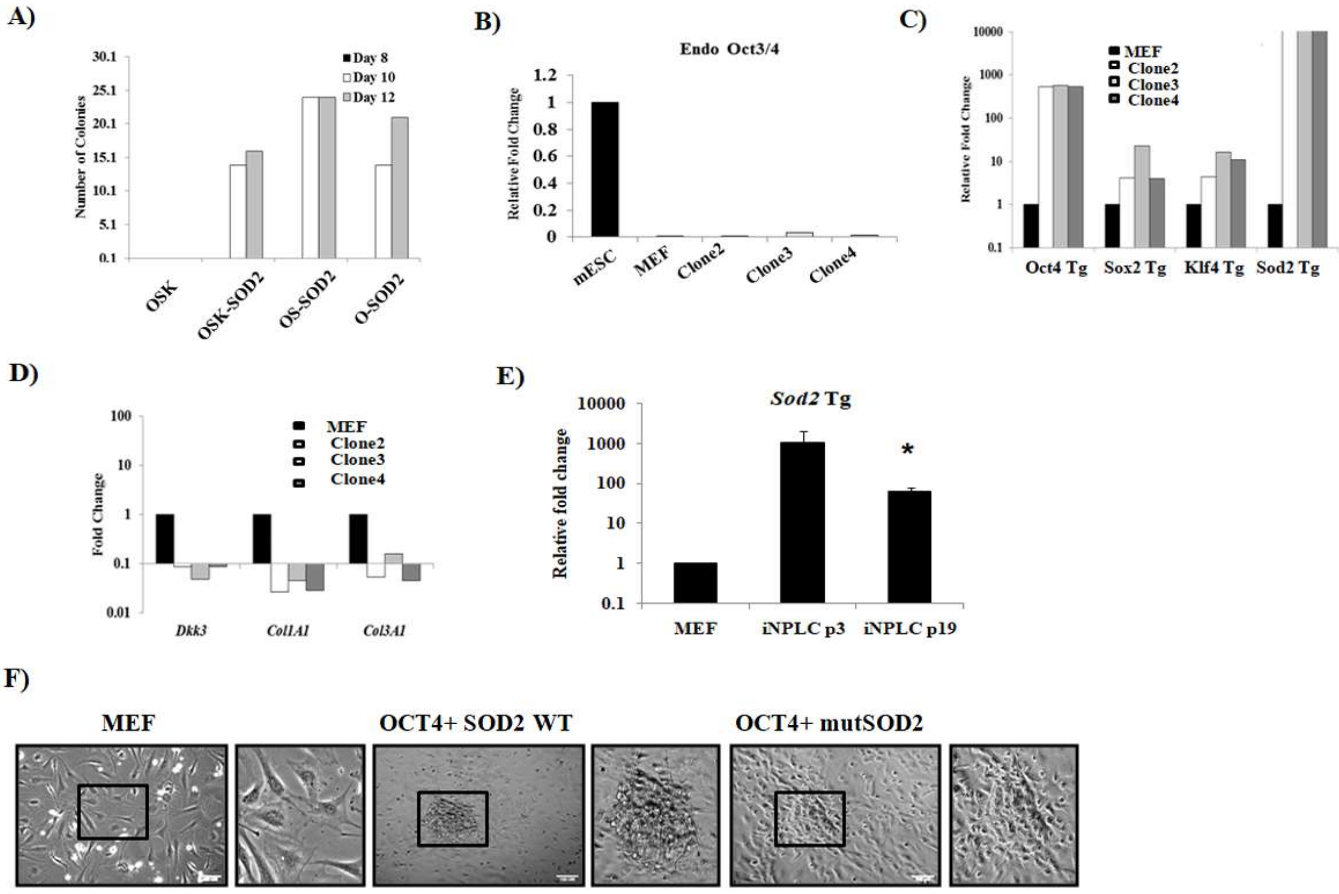

Figure S3, related to figure 3: SOD2 and mutSOD2 mediated transdifferentiation of MEFs to induced neural progenitor like cells (iNPLCs).

(A) Number of colonies developed at day 8, 10 and 12 upon transduction of MEFs with various combinations of reprogramming factors and SOD2.

(B) Transcript analysis of endogenous OCT4 in MEFs and i-NPLC colonies in comparison to mESCs.

(C) Expression of different transgenes in O-SOD2 colonies obtained from MEFs.

(D) mRNA levels of fibroblast markers *Dkk3*, *Col1A1* and *Col3A1* in O-SOD2 clones with respect to starting cell material MEFs.

(E) SOD2 transgene (Tg) expression in MEFs and i-NPLC colonies at passage number 3 and 19.

(F) Phase contrast images of untransduced MEFs and those transduced withOCT4 and SOD2 WT; OCT4 and mutSOD2, cultured in ESC medium. Scale bar represents 100 µm. Data is representative of three individual biological samples. * $p < 0.05$.

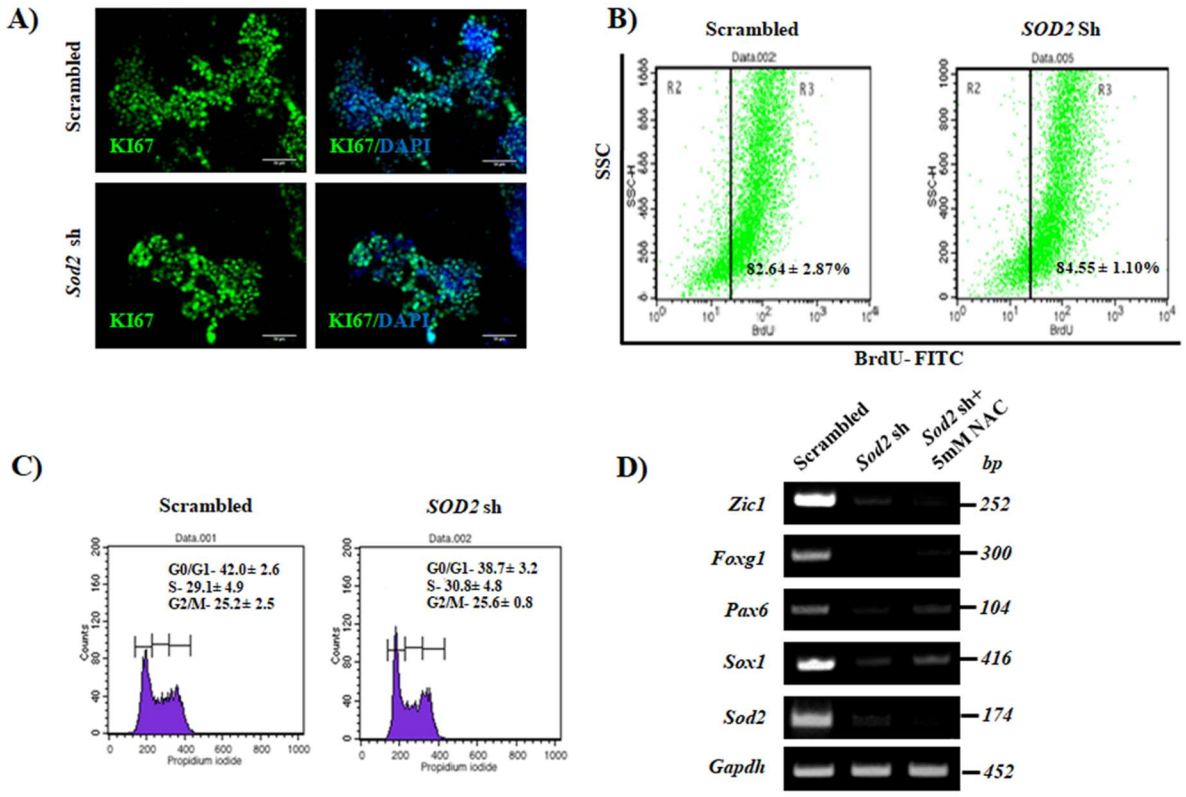

Figure S4, related to figure 4: SOD2 mediated neurogenesis is not due to modulation in cell proliferation or ROS.

(A) Representative immunofluorescence images of Ki67 staining in early neural differentiation of mESCs upon *SOD2* knockdown.

(B) Flow cytometric analysis of BrdU incorporation in early neural differentiation of mESCs upon *SOD2* knockdown.

(C) Cell cycle analysis of early neural differentiation of mESCs upon *SOD2* knockdown.

(D) mRNA levels of early neural markers in neural differentiation with *SOD2* knockdown, and N-acetylcysteine (NAC) treatment with *SOD2* knockdown. Mean ±SE, n= 3 independent experiments.

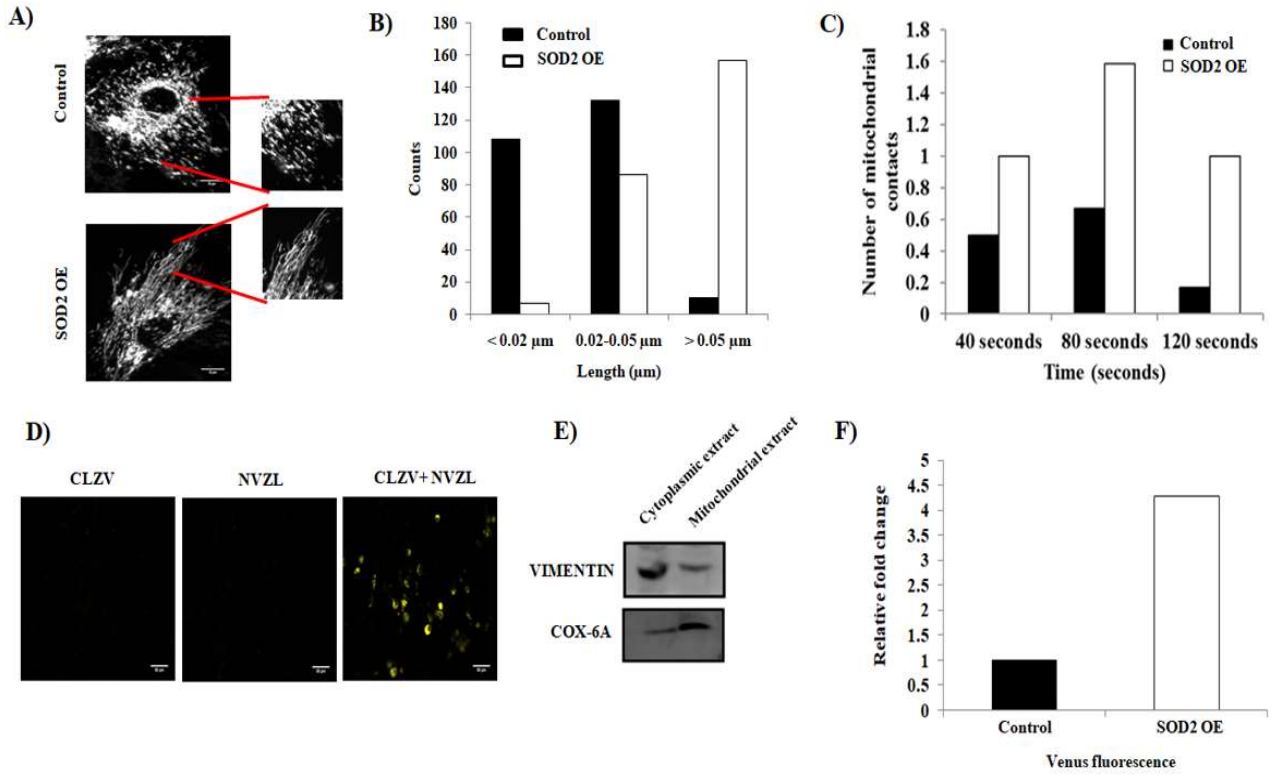

Figure S5, related to figure 5: Over-expression of SOD2 enhances mitochondrial fusion in MEFs.

(A) Representative images of mitochondria in MEFs where SOD2 over-expressed cells show enhanced mitochondrial fusion

(B) Quantification of mitochondrial length upon SOD2 Over-expression in MEFs

(C) Number of mitochondrial contacts at different time intervals in mitochondria of MEFs where SOD2 is over-expressed

(D) Representative image of the MEFs transfected with individual constructs (CLZV and NVZL) or with both the constructs (CLZV+NVZL). Cells transfected with both constructs exhibit Venus fluorescence confirming the bio-complementation process.

(E) Purity of mitochondrial isolation shown by enrichment of mitochondrial specific marker COX-6A in isolated mitochondria

(F) Increase in venus fluorescence indicating mitochondrial fusion upon SOD2 over-expression in MEFs.

Un-cropped full western blot images are available in data S1.

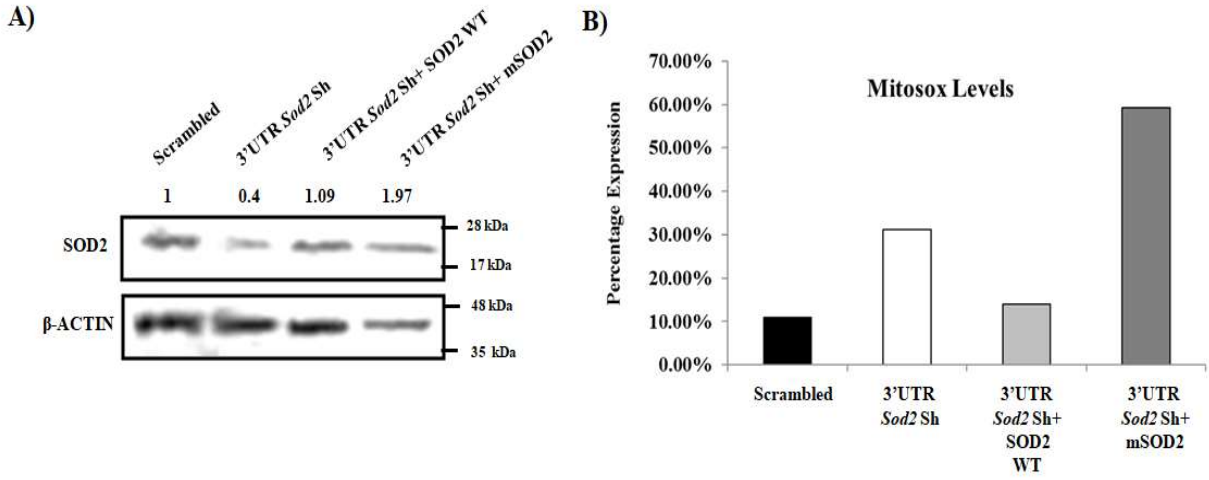

Figure S6, related to figure 5: SOD2 antioxidant mutant hampers the superoxide dismutation by SOD2.

(A) Western blot showing SOD2 expression in cells transduced with scrambled control, 3' UTR *Sod2* sh RNA with and without over-expression of SOD2 WT and mutSOD2. Un-cropped full western blot images are available in data S1.

(B) Mitochondrial superoxide levels measured in mESCs expressing scrambled control, 3' UTR *Sod2* sh RNA with and without over-expression of SOD2 WT and mutSOD2.

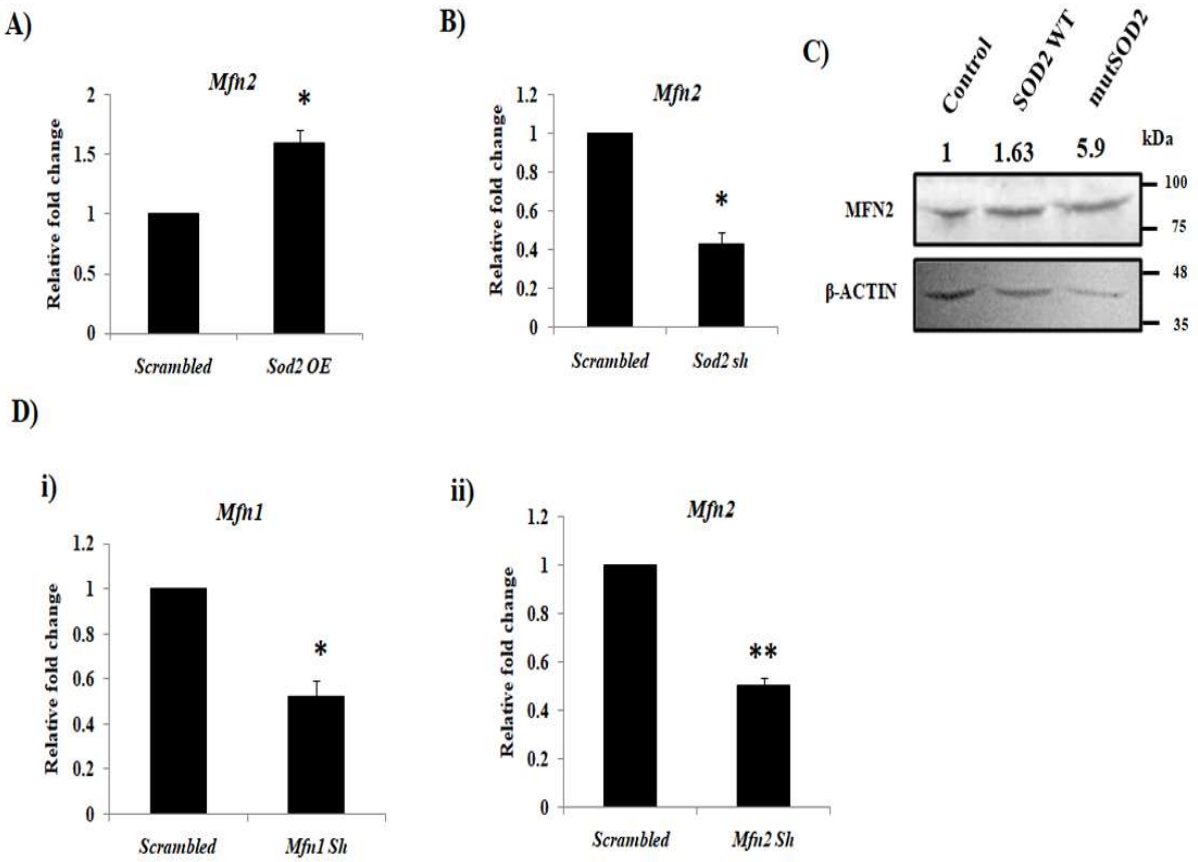

Figure S7, related to figure 6: SOD2 antioxidant mutant has similar effects on MFN2 expression as that of SOD2 WT.

(A and B) Expression analysis of *Mfn2* transcripts upon SOD2 over-expression (A) and knockdown (B).

(C) Western blot showing the effect of SOD2 WT and mutSOD2 over-expression on MFN2 levels.

(D) Knockdown efficiency of *Mfn1* shRNA and *Mfn2* shRNA shown by qPCR. Data is representative of Mean ±SE, n= 3 independent experiments, * $p< 0.05$, ** $p < 0.01$.

Transparent Methods

Ethics Statement

All experiments were approved and performed in compliance with the regulations of the Manipal University Animal ethical Committee and in accordance with the guidelines of the Association for the Assessment and Accreditation of Laboratory Animal Care.

Cell lines and differentiation

mESCs: mouse embryonic stem cells, R1 (a kind gift from Catherine Verfaille, KU Leuven), were cultured on mitotically inactivated mouse embryonic fibroblast (MEF) feeder layer in DMEM high glucose (Gibco) supplemented with 8% FBS (HiMedia), 1X NEAA (Gibco), 1mM GlutaMax (Gibco), 1X Penstrep (Gibco), 1X sodium pyruvate (Gibco) and 100 μM β-Mercaptoethanol (Sigma). To maintain pluripotency, 1000U/mL of LIF (Millipore) was added to the medium. Prior to differentiation, mESCs were cultured on 0.1% gelatin coated dishes for 48 hours.

P40H1 is a hippocampal cell line derived from post natal day 40 mouse. P40H1 cells were cultured in DMEM high glucose supplemented with 5% FBS, 1X NEAA, 1mM GlutaMax and 1X Penstrep.

MEF and HEK293T cells were cultured in medium containing DMEM high glucose with 10% FBS, 1XNEAA, 1mM GlutaMax and 1X Penstrep. The list and specification of the reagents used are provided in Table S2.

Endodermal differentiation

Approximately 2×10^4 cells were plated onto a 12 well plate coated with matrigel in differentiation medium supplemented with 100 ng/mL Activin (Peprotech# 10429- HNAH), 50 ng/mL Wnt3A and 2% FBS. After three days of differentiation, primitive endoderm specific cues were provided. Briefly, 100 ng/mL Activin and 1.5% FBS were supplemented with fresh differentiation medium. Differentiation was terminated on day 6 and the cells were harvested for transcript and protein analyses.

Mesodermal differentiation

mESCs were seeded at a density of 1.5×10^5 cells/sq.cm and maintained in differentiation medium overnight. The medium was then supplemented with10 ng/mL each of EGF (Peprotech# 10605-HNAE), bFGF (Peprotech# 10014- HNAE) and PDGF (R & D systems 220-BB). Differentiation was carried out for 6 days post which the cytokines were withdrawn. The cells were cultured in the medium without cytokines for 4 days to achieve terminal differentiation.

Neural differentiation

mESCs were cultured in N2B27 medium which is a 1:1 mixture of DMEM-F12 with 1X N2 plus supplement (Thermofisher Scientific- #**17502001**)and Neurobasal medium (Gibco) with 1X B27 (Thermofisher Scientific- #12587001) supplemented with 1X Glutamax, 1X Penstrep, 100 µM β-Mercaptoethanol and 10^{-8} M Retinoic acid. The differentiation protocol was staged as early (end of 3 days of differentiation) and late (end of 7 days of differentiation) neural differentiation. The stages were characterized for their efficiency by the respective marker profiles.

Oligodendrocyte differentiation

Cells were seeded at a density of $5*10^4$ cells/cm^2 on ultra-low attachment plates and cultured for 4 days. On day 4 of differentiation, the medium was supplemented with 0.2M retinoic acid (RA). On the next two days, 0.2M RA and 1µM Purmorphamine were added to the differentiation medium. The spheres formed under low attachment were disaggregated and plated on 0.01% polyornithine (Sigma #P4957) coated dishes in differentiation medium DMEM F12, 1X N2 plus supplement, 1mM sodium pyruvate , 1% NEAA, 100 µM β- Mercaptoethanol along with 20 ng/mL bFGF.

Animals

We used 3-4 week old male Swiss Albino mice for mRNA expression analysis of *Sod2* in the whole brain lysate. We used p2 mice to inject iNPLCs labeled with GFP to one of the cortical hemispheres to test their ability to differentiate *in vivo*. The mice post injections were allowed to grow till 4 weeks. Post this, the animals were sacrificed and the brains were harvested for immuno-histochemical analysis.

Western blotting

Cells were lysed with RIPA buffer containing 1X protease inhibitors (Sigma #S8830). The suspension was rocked gently on ice for 20 min and centrifuged at 12000rpm for 15 min. and the clear lysates were stored at -80°C till further use. The samples were prepared by heating with Laemmli buffer at 95°C. Proteins were resolved on a 12% SDS-Polyacrylamide gel and then transferred onto an activated PVDF membrane using a semi-dry blotting apparatus. The non-specific binding on the membrane was blocked with 3% BSA or 3% skimmed milk in 1X TBST. The blots were then incubated with indicated primary antibodies at a concentration of 1:1000 overnight on a rocker at 4^0C. The blots were then washed with 1X TBST thrice and appropriate HRP-conjugated secondary antibodies were added at a concentration of 1:1000. The blots were incubated for 1 hour at room temperature on a rocker and then washed thrice with 1X TBST. The blots were developed using WesternBright ECL HRP susbtrate (Advansta #K-12045-D20) on LI-COR C digit blot scanner. The list and dilutions of primary and secondary antibodies used in this study are provided in Table S2.

qRT-PCR analysis

Cells were lysed with RNAiso Plus (Takara Bioscience) and total RNA was isolated according to the manufacturer's protocol. RNA was quantified by Nanodrop (ThermoScientific Corporation) and 1µg of RNA was converted to cDNA using RevertAid First Strand cDNA synthesis Kit (ThermoScientific Corporation). For transcript analysis, PCR amplification was performed using 2X EmeraldAmp GT PCR Master mix (Takara Biosciences) and the amplified products were visualized on a 2% agarose gel. qPCR analysis was performed using 2X SYBR Green kit (Takara Biosciences) and gene specific primers (Key resource table 1) on a 7500 Real time PCR machine (Applied Biosystems). The list of primers used in this study is provided in Table S1.

Immunofluorescence

Cells were fixed with 4% PFA for 20 min, permeabilized using 0.5% TritonX-100 in PBS for 30 min, and blocked with 20% FBS in PBS for 20 min, at room temperature. Three PBS washes were given after each step. Primary antibodies were added at appropriate concentrations in PBS and incubated at 4^0C overnight. The cells were washed thrice with 1X PBS and incubated with secondary antibodies conjugated with fluorescence tags at a concentration of 1:1000 in room

temperature for 1 hour. List of primary and secondary antibodies used in the study have been provide in Key resource table 2. The cells were counterstained with 1:10000 DAPI for 2 min. After washing with 1X PBS, the cells were visualized under Olympus X73 inverted microscope and images were captured at 20X. Images were pseudo-colored and analyzed using ImageJ software.

Immunohistochemistry:

To track S2 cells injected into infant mouse cortex, we performed IHCs on 4 week old mouse brains. The tissues were fixed with 4% PFA at 4˚C for 72 hours. Cryo-sectioning was performed to obtain 10 µm thick brain sections. The sections were washed once with 1X PBS and incubated with 1:100 primary antibody overnight at 4˚C. Washes were performed with 1X PBS. Secondary antibody was diluted in PBS to a final concentration of 1:600 and the sections were incubated with it for 4 hours at room temperature. The sections were washed thrice with 1X PBS and counter-stained with 1:10000 DAPI. The stained neurons were imaged under 20X objective in Nikon TE 2000 inverted epi-fluorescence microscope.

BrdU incorporation assay

To determine the proliferative status of cells during early neural differentiation, the cells were treated with a final concentration of 10µM BrdU after 18 hours of plating and were differentiated till day 3. After this, the cells were fixed with cold methanol for 15 min at room temperature and then washed thrice with 1X PBS containing 0.1% tween-20 (Sigma) (PBST). Hydrochloric acid, at a working concentration of 2M was added and the samples were incubated at room temperature for 30 minutes. Cells were then permeabilized with 1X BD PermWash for 20 min, blocked with 20% FBS for 30 min at room temperature and incubated with anti-BrdU antibody at a concentration of 1:400 on a rocker at 4^0C overnight. Post washes, the cells were incubated with secondary antibody at a concentration of 1:1000 for 2 hours at room temperature and were analyzed on Flow cytometer for BrdU expression.

Flow cytometry

Cells were trypsinized, washed with 1X Ca^{2+}/Mg^{2+} free PBS, and fixed with 0.1% PFA for 1 hour at room temperature. Post washes with 1X PBS, the cells were permeabilized using BD 1X PermWash and blocked with 20% FBS. Primary antibody was added at a concentration of 1:400

and the cells were incubated on a rocking platform at 4^0C overnight. After three washes with 1X PBS, the cells were incubated with appropriate secondary antibody at a dilution of 1:1000 for one hour at room temperature. The cells were washed thrice with 1X PBS and the events were acquired on BD FACSCalibur analyzer.

DCFHDA staining

Cells were trypsinized and resuspended in serum-free basal medium. DCFHDA (Thermofisher Scientific #D399) was added at a final concentration of 20µM and incubated at 37^0C for 20 min in dark. Events were acquired on BD FACSCalibur to understand ROS levels in mESCs, early neural differentiation and late neural differentiation.

Cell cycle analysis

Cells were trypsinzed and washed once with 1X Ca^{2+}/Mg^{2+} free PBS. The pellet was resuspended in 1mL of hypotonic propidium iodide (PI) solution containing 0.1% sodium citrate, 40µg/mL RNase, 25µg/mL PI and 0.03% NP40 in nuclease free water. The samples were incubated for 10 min on ice in dark and the cell cycle profile was analyzed on BD FACSCalibur.

Transfection and transduction

One day prior to transfection, HEK 293T cells were seeded at a density of $0.2*10^5/cm^2$. The transfection reagent –X-tremeGENE (Merck #6366236001) – was added to OptiMEM (Gibco) at a concentration of 1:4 of the plasmid amount in a sterile polystyrene tube. The tube was thoroughly vortexed for 15 seconds and incubated at room temperature for 10 min. The plasmids of interest, with their respective packaging vectors, were added at recommended concentrations and the tube was vortexed for 15 seconds. The mixture was incubated at room temperature for 20-30 min. and the transfection mixture was added carefully to the cells, which were then incubated at 37^0C with 5% CO_2. The supernatants containing viral particles were collected 48 hours and 72 hours post transfection. Viral particles were concentrated by incubating the supernatants with a final concentration of 50% sterile PEG solution on a rocking platform at 4^0C overnight and then centrifuging at 1600 rpm for 1 hour at 4^0C. The viral pellet was resuspended in minimal volume of basal medium and added to the recipient cells. Cells were provided normal growth medium 24 hours post transduction and selected with 1µg/mL Puromycin wherever applicable. Transduced

cells were further trypsinized and used for different experiments. The list of plasmids used in this study is provided in Table S2.

Derivation and maintenance of O-SOD2 WT and O-mutSOD2 clones

MEFs were transduced with various combinations of retroviral constructs of mOCT4, mSOX2, mKLF4 (kind gift from Dr. Shinya Yamanaka; Addgene #13366, #13367 and #13370 respectively) and pMIG-SOD2 WT. In an independent experiment, MEFs were transduced with mOCT4 and pMIG-mutSOD2. The cells were cultured in mESC medium supplemented with LIF from 48 hours post transduction. After five days of transduction, the cells were trypsinized using 0.25% Trypsin-EDTA Thermofisher Scientific #25200056) and plated on inactivated MEF feeder layer (iMEF) at a density of $0.15*10^6$cells.The medium was changed every alternate day. The colonies were manually picked and then expanded on iMEF feeders.

Differentiation of OS2 cells into mature neurons and glial cells

OS2 cells were cultured in mES-LIF medium (DMEM + 16.6% FBS + 2mM L-Glutamine + 1% Sodium Pyruvate + 0.1M β-mercaptoethanol) on gelatin coated dishes for upto 20 passages, post which they were cultured on matrigel coated plates with Neural Stem Cell medium (DMEM/F12 + 1X N2 + 1X B27 + 80mg Glucose + 0.22% BSA fraction V + 10ng Epidermal Growth Factor + 8ng/mL Fibroblast Growth Factor + 100ng/mL Insulin) before inducing them for neuronal and glial cell differentiation. Media change was given every 2- 3 days and cells post P30 were considered for differentiation.

For neuronal differentiation, 30,000 cells/well were plated onto matrigel coated 12 well plates. After 24 hours of plating, cells were fed with Neural differentiation medium-1 [DMEM/F12 + 1X B27 + 2mM L-Glut + 0.22% BSA fraction V+ 2nM Retinoic Acid + 10uM AraC (Cytosine-B-D-arabinofuranoside hydrochloride) + 10uM Valproic Acid]. Post 72 hrs, the media was changed to Neural differentiation medium-2 (DMEM/F12 + 1X B27 + 2mM L-Glut + 0.22% BSA fraction V + 2nM Retinoic Acid + 5uM AraC + 10uM Valproic Acid) for 3 days. Post 3 days, the cells were cultured in Neural differentiation medium-3 (Electrophys medium, StemCell Technologies with 20ng/mL of BDNF, 20ng/mL GDNF and 10uM Valproic Acid) for 7 days with a media change every 3 days.

For glial differentiation, 5,000 cells/well were plated in Matrigel coated 12 well plates. Post 24 hours of plating, astrocyte differentiation medium was added to the cells (DMEM/F12 + 1X B27 + 2mM L-Glut + 1% FBS). The cells were maintained in the medium for 5 days with media change every 72 hrs before harvesting them for gene and protein expression analysis.

Microarray

The samples for gene expression were labeled using Agilent Quick-Amp labeling Kit (p/n5190-0442). About 500ng each of total RNA were reverse transcribed at 40°C using oligodT primer tagged to a T7 polymerase promoter and converted to double stranded cDNA (ds cDNA). Synthesized ds cDNA were used as template for cRNA generation by *in vitro* transcription and the dye Cy3 CTP (Agilent) was incorporated during this step. Labeled cRNA was cleaned up using QiagenRNeasy columns (Qiagen, #74106) and quality was assessed for yields and specific activity using the Nanodrop ND-1000.

600ng of labeled cRNA sample was fragmented at 60ºC and hybridized on to Agilent's Mouse_GXP_8x60K (AMADID: 28005). Fragmentation of labeled cRNA and hybridization were done using the Gene Expression Hybridization kit (Agilent Technologies, *In situ* Hybridization kit, Part Number 5190-0404). Hybridization was carried out in Agilent's Surehyb Chambers at 65º C for 16 hours. The hybridized slides were washed using Agilent Gene Expression wash buffers (Agilent Technologies, Part Number 5188-5327) and scanned using the Agilent Microarray Scanner (AgilentTechnologies, Part Number G2600D).

Data extraction from Images was done using Feature Extraction software Version 11.5.1.1 of Agilent. Images were quantified using Feature Extraction Software (Version-11.5 Agilent). Feature extracted raw data was analyzed using GeneSpring GX software from Agilent. Normalization of the data was done in GeneSpring GX using the 75th percentile shift and fold expression values were obtained with respect to Specific control Samples. Differential expression patterns were identified among the samples. Significant genes up regulated fold> 1.0 (logbase2) and down regulated <-1.0 (logbase2) in the test samples with respect to control sample were identified. Statistical student T-test was performed and p-value among the replicates was calculated based on volcano plot algorithm. Differentially regulated genes were clustered using hierarchical clustering based on Pearson coefficient correlation algorithm to identify significant

gene expression patterns. Biological analysis was performed for the differentiallyexpressed genes based on their functional category and pathways using Biological Analysis tool DAVID (http://david.abcc.ncifcrf.gov/).

SOD2 activity assay

Cells were harvested and the protein concentrations were determined using BCA estimation kit (Novagen, USA) with BSA as the standard. Equal amounts of protein from each sample were taken to assess SOD2 activity using a colorimetric method, according to manufacturer's instructions (Biovision #K335). Briefly, the samples were incubated with WST solution followed by the addition of dilution buffer. Release of superoxide was initiated by addition of enzyme working solution and the samples were incubated for 20 minutes at 37^0C. Absorbance was recorded at 450nm using Ensightmultiwell plate reader and SOD2 activity was calculated.

Mitochondrial superoxide staining

Cells were trypsinized, washed once with 1X PBS to remove traces of FBS and resuspended in serum free basal medium. Mitosox red (Thermofisher Scientific #M36008) was added to the suspension at a final concentration of 20 μM. The samples were incubated at 37^0C in dark for 20 min. The cells were washed once with basal medium and the events were acquired on BD FACS Aria II.

Mitochondrial length and contact measurement

Mitochondria were labeled by transiently transfecting P40H1 cells with pLVmitoDsred construct (addgene 44386) and imaged using Olympus FV3000 inverted microscope at 63X magnification or Olympus X73 inverted microscope at 20X magnification. Images were processed using ImageJ software. The length of mitochondria was measured using line tool in ImageJ and tabulated. The number of mitochondrial kiss and run events were counted across different time frames using the live videos captured with DsRed labeled mitochondria.

shRNA cloning

Oligonucleotides (Supplementary table 1) of mouse *Sod2*, *Mfn1*and *Mfn2* were procured and allowed to anneal with respective reverse complimentary sequences a 95^0C for 5 min. The reaction mixture was slowly cooled down to room temperature and then transformed to DH5α competent cells along with the pLKO 1.puro lentiviral vector backbone digested with AgeI and EcoRI. Plasmid was isolated from the colonies obtained and sequenced for the selection of positive clones.

For *Sod2* inducible shRNA cloning, the annealed oligonucleotides were cloned into Tet- pLKO-puro vector.

Cloning SOD2 over-expression construct

SOD2 CDS was amplified from mESCcDNA using PhusionTaq polymerase enzyme and cloned into pMIG MCS IRES GFP backbone. The clones obtained were confirmed by DNA sequencing.

Generation of SOD2 antioxidant mutant clone

Point mutations were introduced in SOD2 sequence so that the protein formed is incapable of quenching mitochondrial superoxide. Two such mutations were performed to convert D-183 to N-183 and W-185 to F-185. The template selected was pMIG-Sod2-IRES-GFP. In order to generate site specific mutagenesis, this WT plasmid was amplified using sense and antisense oligonucleotides containing mutations and a *MluI* restriction site for the ease of screening positive clones. The oligonucleotides were 5' – GCTGGGGATTAACGTGTTTGAGCACGCGTACTACC-3' and 5' – GGTAGTACGCGTGCTCAAACACGTTAATCCCCAGC – 3'. The clones obtained were digested with methylation dependent restriction enzyme *DpnI* for the removal of WT SOD2 template and transformed using DH5-α. The colonies were screened for the positive clone by restriction digestion of the plasmid with *MluI* and were confirmed further by DNA sequencing.

Isolation of mitochondria

Cells were washed once with ice-cold 1X PBS, scrapped on ice, transferred to a chilled microcentrifuge tube and spun at 800g for 5 min at 4^0C. The cell pellet was resuspended in 3mL of ice cold Isolation Buffer c (IBc-10mM Tris-base, 1mM EGTA< 0.2M Sucrose at pH 7.4) and

homogenized using a pre-chilled Teflon dounce homogenizer. The homogenate was spun at 600g for 10 min at 4^0C. The supernatant was collected and centrifuged at 7000g for 10 min at 4^0C. The supernatant was discarded and the pellet was washed with 200µL of ice cold IBc and spun at 7000g for 10 min at 4^0C. The mitochondrial pellet was resuspended in minimal volume of IBc and further used for mitochondrial fusion assay.

Mitochondrial fusion assay

Mitochondrial fusion assay was performed as previously published (Schauss*et.al.,* 2010) with some modifications. Briefly, the mitochondria were isolated from two different populations of cells each harboring one half of venus and luciferase construct that is targeted to mitochondria. The mitochondrial pellets were resuspended in a reaction buffer containing 10 mM HEPES (pH 7.4), 110 mMMannitol, 68 mM Sucrose, 80 mMKCl, 0.5 mM EGTA, 2 mM Mg $(CH_3COO)_2$, 0.5 mM sodium succinate and 1 mM DTT. The mitochondria were then concentrated by centrifuging at 9000g for 1 min. The samples were incubated on ice for 30 min, then resuspended in the reaction buffer, and further incubated on ice for 30 min. Mitochondria were resuspended and warmed to 37^0C for 10 min, resuspended in minimal volume of the reaction buffer, and venus fluorescence was recorded at 515 nm $_{(Exc)}$ and 530 nm $_{(Emi)}$.

Quantification and Statistical Analysis

Image analysis and quantification of mitochondrial length and contacts was performed on ImageJ software.

Adobe photoshop was used to prepare figures with 300 dpi resolution.

Statistical analysis was performed using a two-tailed Student t-test. P values of $p \leq 0.05$ (*) were considered significant; $p \leq 0.005$ (**) and $p \leq 0.001$ (***) were considered highly significant.

Table S1: Primer sequences used for transcript analysis related to Figure 1, Figure 2, Figure 3, Figure 4, Figure 6, Figure S1, Figure S2, Figure S3, Figure S4, Figure S5, Figure S6 and Figure S7.

Primer Name	Sequence	Amplicon size (bp)
Gapdh	Forward primer: ACCACAGTCCATGCCATCAC Reverse primer: TCCACCACCCTGTTGCTGTA	452
Oct4	Forward primer: GAGGAGTCCAGGACATGAA Reverse primer: AGATGGTGGTCTGGCTGAAC	153
Map2	Forward primer: TCAGGAGACAGGGAGGAGAA Reverse primer: GTGTGGAGGTGCCACTTTTT	112
Sod2	Forward primer: CCGAGGAGAAGTACCACGAG Reverse primer: GCTTGATAGCCTCCAGCAAC	174
Sod1	Forward primer:CGGTGAACCAGTTGTGTTGT Reverse primer: AGTCACATTGCCCAGGTCTC	190
Pax6	Forward primer: TCCCAGGGATCTGAGAATTG Reverse primer: CACAACGGTTTGAAATGACG	104
Mog	Forward primer: ACCAAGAAGAGGCAGCAATG Reverse primer: GGTCCAAGAACAGGCACAAT	259
Olig2	Forward primer: CAGCGAGCACCTCAAATCTA Reverse primer: CACAGTCCCTCCTGTGAAGC	199
Foxg1	Forward primer: ACCTGTCCCTCAACAAGTGC Reverse primer: ACGTGGTCCCGTTGTAACTC	300
Pdgfr-a	Forward primer: CACACCGGATGGTACACTTG Reverse primer: GGCAGAGTCATCCTCTTCCA	159
Sox1	Forward primer: CTGCTCAAGAAGGACAAGTA Reverse primer: CTCATGTAGCCCTGAGAGT	416
Zic1	Forward primer: GCCCTTCAAAGCCAAATACA Reverse primer: TTGCAAAGGTAGGGCTTGTC	252
Tuj1	Forward primer: TAGACCCCAGCGGCAACTAT	127

	Reverse primer: GTTCCAGGTTCCAAGTCCACC	
N-Caherin	Forward primer: GATTTCAAGGTGGACGAGGA Reverse primer: CACTGTGCTTGGCAAGTTGT	223
Mixl1	Forward primer: CTACCCGAGTCCAGGATCCA Reverse primer: ACTCCCCGCCTTGAGGATAA	101
Vimentin	Forward primer: AGAGAGGAAGCCGAAAGCA Reverse primer: CTTTCATACTGCTGGCGCAC	248
Sox17	Forward primer: CACAACGCAGAGCTAAGCAA Reverse primer: TTGTAGTTGGGGTGGTCCTG	128
Cxcr4	Forward primer: GTGCAGCAGGTAGCAGTGAC Reverse primer: GGCAGGAAGATCCTGTTGAA	207
Foxa2	Forward primer: CCCGGGACTTAACTGTAACG Reverse primer: TCATGTTGCTCACGGAAGAG	152
NeuN	Forward primer: GCACAGACTCATCCTGAGCA Reverse primer: GGTGGAGTTGCTGGTTGTCT	115
Nurr1	Forward primer: AGTCTGATCAGTGCCCTCGT Reverse primer: GATCTCCATAGAGCCGGTCA	162
Tau	Forward primer: GGTCCATGTCTCCTTCTTGG Reverse primer: TCTTCTGTCCTCGCCTTCTG	132
Gata6	Forward primer: CAACACAGTCCCCGTTCTTT Reverse primer: TGGTACAGGCGTCAAGAGTG	122
Flk1	Forward primer: CCCGCATGAAATTGAGCTAT Reverse primer: AAACATCTTCGCCACAGTCC	175
Vegf	Forward primer: CTGCTCTCTTGGGTGCACTG Reverse primer: TTCACATCTGCTGTGCTGTAG	375
Otx2	Forward primer: GGAAGAGGTGGCACTGAAAA Reverse primer: ACTGGCCACTTGTTCCACTC	188
P75	Forward primer: GCTCAGGACTCGTGTTCTCC Reverse primer: TGGCTATGAGGTCTCGCTCT	285
Plzf	Forward primer: GTGCCCAGTTCTCAAAGGAG	131

	Reverse primer: CTCCATGTGCTGCTGGAGT	
Gfap	Forward primer: GGAGAGGGACAACTTTGCAC Reverse primer: TCCAGCGATTCAACCTTTCT	165
S100β	Forward primer: GGTGACAAGCACAAGCTGAA Reverse primer: GTCCAGCGTCTCCATCACTT	120
Mfn1	Forward primer: ATTGGGGAGGTGCTGTCTC Reverse primer: TCAGGAAGCAGTTGGTTGTG	142
Mfn2	Forward primer: TCCAAGGTCAGGGGTATCAG Reverse primer: CAATCCCAGATGGCAGAACT	133
Nestin	Forward primer: CTGCAGGCCACTGAAAAGTT Reverse primer: GTGTCTGCAAGCGAGAGTTC	187
Dkk3	Forward primer: GGAGGAAGCTACGCTCAATG Reverse primer: CGTGCTGGTCTCATTGTGAT	175
Col1A1	Forward primer: GCCAAGAAGACATCCCTGAA Reverse primer: TCTTCATTGCATTGCACGTC	142
Col3A1	Forward primer: GCACAGCAGTCCAACGTAGA Reverse primer: TCTCCAAATGGGATCTCTGG	185
Mfn1 sh RNA	CCGGTACGGAGCTCTGTACCTTTATCTCGAGATAAAGGTAC AGAGCTCCGTATTTTTG	
Mfn2 sh RNA	CCGGGGCAGTTTGAGGAGTGCATTTCTCGAGAAATGCACT CCTCAAACTGCCTTTTTTG	
SOD2 3'UTR sh RNA	CCGGCCCAAACCTATCGTGTCCATTCTCGAGAATGGACAC GATAGGTTTGGGTTTTTG	
SOD2 inducible sh RNA	CCGGGAGGCTATCAAGCGTGACTTTCTCGAGAAAGTCACG CTTGATAGCCTCTTTTTG	

Table S2: List of antibodies used for protein expression analysis related to figure 1, figure 2, figure 3, figure 4, figure 6, figure S1, figure S2, figure S4, figure S5, figure S6 and figure S7; chemicals used for cell culture and differentiation; plasmid constructs used for retroviral and lentiviral transductions.

REAGENT OR RESOURCE	SOURCE	IDENTIFIER
Antibodies		
Mouse anti β-ACTIN	Santa Cruz	#sc-47778
Rabbit anti NUCLEOLIN	Sigma aldrich	#N2662
Rabbit anti SOD2	EMD Millipore	# AB10346
Rabbit anti SOX1	Abcam	# ab109290
Rabbit anti FOXG1	Abcam	#ab18259
Rabbit anti MFN1	Cloudclone	PAC619Mu01
Rabbit anti MFN2	CST	mAB #9482
Mouse anti BrdU	DSHB	#G3G4
Mouse anti NESTIN	BD Pharmingen	#556309
Rabbit anti COX 6A	CusaBio	#CSB-PA637381XA01CXY
Rabbit anti FIS1	CusaBio	#CSB-PA008684LA01HU
Mouse anti PAX6	DSHB	#DSHB-S1-1281
Rabbit anti ZIC1	Abcam	#ab134951
Rabbit anti OLIG2	Abcam	#ab81093
Rabbit anti VIMENTIN	CusaBio	#CSB-MA000319
Mouse anti NF200 kDa	Abcam	#ab40796
Mouse anti SYNAPTOPHYSIN	Novus Biologicals	#NB300-653SS
Mouse anti S100β	BD Biosciences	#612376

Rabbit anti GFAP	BD Biosciences	#610565
Rabbit anti TUJ1	Abcam	#ab18207
Mouse anti KI67	BD Pharmingen	#550609
Rabbit anti-mouse FITC	SigmaAldrich	#AP160F
Goat anti Mouse AF594	ThermoFisher Scientific	#11005
Donkey anti-Rabbit AF594	ThermoFisher Scientific	#21207
Donkey anti-Rabbit AF488	ThermoFisher Scientific	#21206
Plasmid Constructs		
pMIG-SOD2-IRES-GFP WT	In-house	
pMIG-SOD2-IRES-GFP mutant	In-house	
pLKO-mSod2 shRNA	Sigma Aldrich	TRCN0000324404
pLKO-mMnSOD/Sod2 3'UTR shRNA	In-house	
Sod2 sh RNA tet inducible	In-house	
Sod2 tet inducible	In-house	
Mfn1 sh RNA	In-house	
Mfn2 sh RNA	In-house	
pQCXIP-C-Mito luciferase Zipper Venus (C-mito LZV)	Prof. Heidi McBride's lab	
pQCXIP-N-Mito Venus Zipper luciferase (N-mito VZL)	Prof. Heidi McBride's lab	
pLV mito dsRed	Addgene	#44386

Chemicals and Reagents	Source	Identifier
BMP4	ThermoFisher Scientific	PHC9533
Retinoic acid	Merck	R2625- 100MG
GDNF	R&D systems	212-GD-01M
BDNF	R&D systems	248-BDB
EGF	Peprotech	315-09
FGF-2	Peprotech	100-18B
Cytosine-B-D-arabinofuranoside hydrochloride	SigmaAldrich	C6645
Valproic acid	SigmaAldrich	P4543-10G
N-acetyl cysteine	Merck	A7250-25G
BSA Fraction V	SigmaAldrich	# 10735086001
LIF	Merck	ESG1106
DMEM F12	Gibco	# 11320-033
DMEM HighGucose	Gibco	# 11965-092
Neurobasal medium	Gibco	# 38210000
NEAA	Gibco	# 11140-050
L-GlutaMax	Gibco	# 35050-061
Anti anti	Gibco	# 15240062
Sodium Pyruvate	Gibco	# 11360070
β-Mercaptoethanol	Sigma	# M7522
N2 plus supplement	Invitrogen	# 17502048
B27 without Vitamin A	Invitrogen	# 12587-010
FBS	HiMedia	RM9951